Vol. 12(9), pp. 335-356, September 2018
DOI: 10.5897/AJEST2018.2515
Article Number: A66FA3F58469
ISSN: 1996-0786

http://www.academicjournals.org/AJEST

African Journal of Environmental Science and Technology

Full Length Research Paper

Equilibrium, kinetic and thermodynamic studies of biosorption of zinc ions from industrial wastewater using derived composite biosorbents from walnut shell

Olafadehan, O. A.[1*], Akpo, O. Y.[1], Enemuo, O.[1], Amoo, K. O.[1] and Abatan, O. G.[2]

[1]Department of Chemical and Petroleum Engineering, University of Lagos, Akoka-Yaba, Lagos, Nigeria.
[2]Department of Chemical Engineering, Covenant University, Canaan Land, Ota, Ogun State, Nigeria.

Received 28 May, 2018; Accepted 6 June, 2018.

The biosorption process of Zn (II) ions in industrial wastewater was investigated using derived composite biosorbents from walnut and snail shells. Composite adsorbents were produced by activating walnut shell carbon (WSC) with phosphoric acid to obtain acid-treated walnut shell carbon (AWSC) and WSC and AWSC were independently impregnated on chitosan to produce walnut shell carbon impregnated on chitosan (WSCC) and acid-treated walnut shell carbon impregnated on chitosan (AWSCC) respectively. The removal efficiencies of Zn (II) ions from synthetic wastewater using the prepared adsorbents were determined. The effects of operational parameters on Zn (II) ions adsorption were investigated. The adsorption data of Zn (II) ions were analysed using Langmuir, Freundlich and Temkin isotherms. The Langmuir isotherm fitted the adsorption data excellently for the derived composite biosorbents, giving an indication of monolayer coverage on the derived composite biosorbents and the determination coefficients were close to unity. Also, the maximum adsorption capacities of 3.1104, 3.8052, 16.4474 and 17.6991 mg/g were obtained for WSC, AWSC, WSCC and AWSCC at pH=5, 1 g of adsorbent dosage, Zn (II) ions initial concentration of 30 mg/L, contact time of 2 h, agitation speed of 150 rpm, particle size of 60 BSS and temperature of 30°C. The kinetic modelling of Zn (II) ions adsorption showed that pseudo second-order kinetic model gave the best fit amongst the investigated kinetic models. The adsorption of Zn (II) ions on the prepared adsorbents was film-diffusion controlled. The experimental results of this study showed that acid-treated walnut shell carbon impregnated on chitosan has the potential to be applied as alternative efficient low-cost biosorbent in the remediation of heavy metal contamination in wastewater. The thermodynamic parameters indicated that the adsorption of Zn (II) ions on the derived composite biosorbents was exothermic, endogonic, favourable, non-spontaneous with changes in enthalpy (ΔH, negative), entropy [ΔS, nearly zero (though negative)], and Gibbs free energy (ΔG, positive), for all the prepared adsorbents.

Key words: Adsorption, biosorbents, chitosan, isotherm, kinetic models, film diffusion.

INTRODUCTION

Water pollution is one of the major problems faced globally due to the random release of domestic and urban wastewaters, agricultural wastes and industrial effluents into water courses. The main impact of such pollution is the enormous amount of heavy metals (such as nickel, lead, copper, zinc, cadmium, etc) in effluents released by industries like electroplating, plastic and paint manufacturing, mining and metallurgical processes, pulp and paper, petrochemical and battery manufacturing industries (Oboh et al., 2009). These metals are toxic and

non-biodegradable, and can cause environmental pollution. Moreover, human health can be adversely affected as these metal ions are highly soluble in water and can be absorbed into the body. Hence, removal of these heavy metals from wastewater is essential for the purpose of protecting the environment and human health.

Trace concentrations of zinc are important for the physiological functions of living tissue and regulation of many biochemical processes. However, like other heavy metals, when zinc is discharged into natural waters at increased concentrations from industries involved in acid mine drainage, galvanizing plants, natural ores and municipal wastewater treatment plants, it can have severe toxicological effects on humans and aquatic ecosystems (Aremu et al., 2002). Zinc is non-biodegradable and it travels through the food chain via bioaccumulation. World Health Organization recommended the maximum acceptable concentration of zinc in drinking water as 5.0 mg/L (Hawari et al., 2009).

The orthodox treatment techniques for the heavy metals removal from industrial wastewater include chemical precipitation, membrane filtration, electrolytic reduction, solvent extraction, ion exchange, electro-dialysis, ultra filtration and adsorption on activated carbon (Bhattacharyya et al., 2009; Amadi and Ukpaka, 2015; Babarinde et al., 2016; Babarinde and Onyiaocha, 2016; Iqbal, 2016; Iqbal and Bhatti, 2015b; Iqbal and Khera, 2015; Iqbal and Nisar, 2015; Iqbal et al., 2017; Jamal et al., 2015; Nouren et al., 2017; Patel et al., 2017; Qureshi et al., 2015; Sayed, 2015; Ukpaka and Izonowei, 2017; Ukpaka and Igwe, 2017). However, adsorption has been recognised as a viable technique for removal of heavy metal ions from wastewater (Adesola et al., 2016; Babarinde and Onyiaocha, 2016; Iqbal and Bhatti, 2015a; Iqbal et al., 2016; Iqbal and Khera, 2015; Mushtaq et al., 2016; Rashid et al., 2016) owing to its simplicity, cost effectiveness and feasibility (Foo et al., 2010).

Activated carbon is the most important adsorbent used industrially for the separation and purification of products and also for the treatment of liquid and gaseous effluents owing to its porous surface area, controllable pore structure, thermo-stability and low acid/base reactivity (Mohan et al., 2007). Despite its use in adsorption processes, the biggest barrier in its application by industries is its costly nature and the tediousness of its manufacturing and regeneration processes. Consequently, relatively low cost adsorbents from biomass, called biosorbents, have been developed. Examples of some biological materials used as biosorbents are rice straw, coconut shell, walnut shell, banana pith, beech leaves, orange peels, moss, tree fern, soya cake, cactus leaves and carbonized biomass products (Bhattacharyya et al., 2004). Moreover, Kauser et al. (2017) compared batch and column adsorption studies for the uranium (VI) ions adsorption onto rice husk waste biomass (RHWB) and concluded that RHWB had potential for removing uranium (VI) ions with batch adsorption more efficient than the column mode. Naeem et al. (2017) carried out uranium adsorption using modified low cost *Vigna radiata* biomass, with maximum uranium removal of 230 mg/g obtained at the optimized process parameters of pH=4, biosorbent dose of 0.05 g, contact time of 60 min and temperature of 40°C using 400 mg/L uranium ions concentration. Akram et al. (2017) showed the efficacy of the prepared biocomposite of mango (*Mangifera indica*) with surfactants and co-metal ions (Na^+, K^+, Ca^{2+}, Cu^{2+}, Al^{3+} and Fe^{3+}) for Cr (VI) ions removal from industrial effluents. They also obtained optimum levels of process variables of pH, Cr(VI) ions initial concentration, adsorbent dosage, contact time and temperature as 3, 0.05 g, 30 min, 200 mg/L and 33 °C, respectively for maximum Cr (VI) adsorption onto the prepared biocomposite.

Zarur et al. (2018) investigated the use of agroindustrial waste, corn husk biomass (*Zea mays*) as adsorbent for the removal of Cr (VI) and Hg (II) ions, with a view to carrying out thermodynamic, kinetic and equilibrium studies of the process. In their work, Elovich kinetic model and Freundlich isotherm correlated the experimental data excellently, and the therodynamic parameters (ΔH^0, ΔG^0 and ΔS^0) suggested a favourable, spontaneous, reversible and endothermic removal process.

Biosorption can be defined as the passive and non-metabolically simplified process of metal ion binding by dead biomass (Kumar et al., 2006). It is effective, flexible and can remove large amounts of heavy metal ions from industrial effluent using a very simple and straight-forward method. Moreover, it is beneficial to the environment as pollutants from both aqueous and gaseous streams can be effectively removed with minimum sludge discharge. Furthermore, biosorption produces treated wastewater of higher purity as compared with the conventional metal removal methods (Kumar et al., 2006). Other advantages of biosorption include high versatility, metal selectivity and overall performance with no concentration dependence, no nutrient requirements, high tolerance for organics and possibility of biosorbent regeneration and reuse (Volesky, 1990). Biosorption is also cost effective as raw materials can be obtained easily in large quantities, mostly from natural or waste materials (Dash, 2010). Therefore, biosorption technology has become an attractive

*Corresponding author. E-mail: oolafadehan@unilag.edu.ng. Tel: +234802 912 9559.

alternative for wastewater treatment today.

Biomaterials from agricultural operations have potential to be used as low-cost adsorbents since they are unused, are widely available and environmentally friendly resources (Deans and Dixon, 1992). Walnut shell (*Tetracarpidium conophorus*) is a highly carbonaceous and fibrous material with little or no economic value, and its abundance and low cost makes it a good source for the production of activated carbon. Its disposal is not only costly but also causes environmental problems. Hence, the production of char from walnut shells adds value to the walnut shells. It also helps to reduce the cost of waste disposal, and provides a potentially cheap alternative to the commercial carbonaceous adsorbents (Logan and Rosemarie, 2002). Ahlam et al. (2012), Firas and Aurelia (2015), Ghasemi et al. (2015) and Mahboobeh et al. (2012) have reported processing of walnut shells into char for the treatment of industrial and municipal wastewaters.

Amongst the low cost adsorbents, chitosan possesses the highest sorption capacity for several metal ions (Babel and Kurniawan, 2004; Nomanbhay and Palanisamy, 2005). Chitin, 2-acetamido-2-deoxy-β-D-glucose-(N-acetylglucan), is the second most abundant polymer in nature. It occurs in nature as ordered crystalline micro fibrils forming structural components in the exoskeleton of anthropoids (Rinaudo, 2006); its major source is from exoskeleton of sea foods (crab, shrimp, prawn, and lobster shells) that are usually disposed as waste material. Depending on its source, three different crystalline polymorphic forms of chitin have been identified: α-chitin (shrimp and crab shells), β-chitin (squid pen), and γ-chitin (stomach cuticles of cephalopoda) (Jang et al., 2004). Chitosan, 2-acetamido-2-deoxy-β-D-glucose-(N-acetylglucosamine), is a biopolymer with free amine groups that are suitable for the adsorption of heavy metals. It is produced on an industrial level by chemical deacetylation of chitin with NaOH. Chitosan can also be produced by enzymatic deacetylation of chitin using lysozyme, snailase, neutral protease, and chitin deacetylase (Cai et al., 2006). Chitosan is slightly soluble at low pH values and poses problems for development in commercial applications. The active binding sites of chitosan are not readily available for sorption. The sites are reported to be soft and have a tendency to agglomerate or form gel in aqueous solutions. Transport of metal contaminants to the binding sites plays a very significant role in process design. Therefore, it is imperative to provide physical support and increase the accessibility of the metal binding sites for process applications (Amuda et al., 2007; Nomanbhay and Palanisamy, 2005). Some investigators (Bamgbose et al., 2010; Karthikeyan et al., 2004; Muzzarelli, 1977; Schmuhl et al., 2001; Vold et al., 2003; Wana et al., 2010) have reported the use of chitosan as adsorbent for the treatment of industrial and municipal wastewaters. However, impregnation of either char obtained from carbonaceous materials or of activated carbon on chitosan (Amuda et al., 2007; Ding et al., 2006; Nomanbhay and Palanisamy, 2005; Wu et al., 2002) has resulted in a diversity of adsorbents with far superior adsorption capacity.

The objectives of this study were to prepare char from walnut shell, perform surface modifications of the walnut shell carbon (WSC) via chemical activation using phosphoric acid to obtain acid-treated walnut shell carbon (AWSC), and the respective impregnation of WSC and AWSC on chitosan to obtain walnut shell carbon impregnated on chitosan (WSCC) and acid-treated walnut shell carbon impregnated on chitosan (AWSCC) with a view to investigating the respective removal efficiencies of Zn (II) ions in aqueous solutions using the prepared adsorbents. The effects of solution pH, adsorbent dosage, initial metal ion concentration, contact time, agitation speed and temperature on the percentage removal of Zn (II) ions in industrial wastewater were also investigated. Three adsorption isotherms (Langmuir, Freundlich and Temkin) and five kinetic models were used to analyse the equilibrium adsorption data and the kinetic data of Zn (II) ions removal respectively. Thermodynamic studies of the Zn (II) ions adsorption on the prepared biosorbents were carried out to determine the spontaneity, exothermic or endothermic nature of the process, and its feasibility.

MATERIALS AND METHODS

All the chemicals used were of analytical grade, purchased from Sigma Aldrich in Germany and used as received. These included zinc (II) tetraoxosulphate heptahydrate ($ZnSO_4.7H_2O$) (99%) for the synthesis of the industrial wastewater, NaOH (98%) and hydrochloric acid (99%) for the preparation of chitosan, and oxalic acid (99.9%) for the preparation of chitosan gel.

Preparation of char from walnut shell (WSC)

The locally purchased walnut shells were cleaned and washed several times with distilled water to remove surface impurities. After drying, the shells were crushed. To prevent a sticky effect in screening, the samples were dried in an oven at 105°C till constant mass for 4 h prior to screening. The dried shells were screened (sieved) into different particle sizes of 0.80, 0.45, 0.25, 0.20 and 0.15 nm and stored in plastic air-tight containers. The carbonization process was carried out as previously described by Amuda and Ibrahim (2006). The equation for carbonization process is shown thus:

$$\text{Walnut shell} \xrightarrow{600^{o}C,\ 2h} \text{WSC} + CO_2 \quad (1)$$

Preparation of acid-treated walnut shell carbon (AWSC)

The activation of the walnut shell carbon (WSC) using phosphoric acid was carried out by the method previously described by Idowu (2015) with a slight modification. Exactly 30 g of the carbonized walnut shell was weighed into a crucible and mixed with 1 M H_3PO_4. The crucible with its content was heated at 750°C or a period of 5

min. The activated sample was allowed to cool to ambient temperature; the samples were washed several times with deionized water until pH 6-7, filtered with Whatman No. 1 filter paper (150 mm diameter, Cat No. 1001 150) and dried at 110°C for 4 h. The chemical equation for the activation process is shown thus:

$$\text{WSC} \xrightarrow{750^{o}C,\ H_3PO_4,\ 5\text{min}} \text{AWSC} + CO_2 \quad (2)$$

Preparation of chitin from snail shell

Snail shells were ground to a smaller particle size, pulverized and screened to a particle size of 1 mm. The method reported by Mohanasrinivasan et al. (2014) was employed for the preparation of chitin with slight modification. 80 g of the powder was mixed with 100 mL of 4 wt% NaOH. The mixture was boiled and stirred at 100°C for 2 h in a water bath. It was then filtered and washed with distilled water. Red litmus was used to check if the base was completely washed away. After washing, the mixture was filtered and the residue was dried at 100°C for 3 h. After deproteinatization, the weight of the sample was 62 g. 30 mL of 5 wt% 1 M HCl was added to the deproteinized sample. The mixture was boiled and stirred for 45 min at 100°C in a water bath in order to remove all mineral materials (mainly $CaCO_3$). Subsequent washing was done with distilled water followed by filtration. The mixture was examined with blue litmus to check the acidity of the mixture. The residue (chitin) obtained was dried in the oven at 100°C for 2 h.

Preparation of chitosan

Deacetylation reaction was used to convert chitin to chitosan according to a revised procedure of Coughlin et al. (1990). Then, a method described by Nomanbhay and Palanisamy (2005) was used for the preparation of chitosan gel. The degree of deacetylation of chitosan was determined by applying the method used by Guibal et al. (1994). The molar mass of chitosan was determined by using the equation of Mark-Houwink-Sakurada for viscosity measurements at different concentrations, given by Paul and Lodge (2007):

$$\eta = kM^{\alpha_1} \quad (3)$$

Where, η and *M* are the respective intrinsic viscosity and molecular weight of chitosan, *k* and α_1 are the Mark-Houwink Sakurada constants for a given polymer-solvent temperature system.

Surface modification of WSC and AWSC with chitosan

The surface modification of WSC and AWSC with chitosan gel was carried out using the method described by Babel and Kurniawan (2004). 50 g of the AWSC was slowly added to 100 ml of chitosan gel diluted with 500 ml of water and heated to 50°C and then agitated at 150 rpm for 6 h. The prepared AWSCC was washed with deionized water and dried at 102°C for 2 h. The same process was applied to WSC to obtain walnut shell carbon impregnated on chitosan (WSCC). The AWSCC and WSCC were then soaked in 0.5% NaOH solution till any residual acid was removed. Both adsorbents were rinsed extensively with deionized water and dried in an oven at 102°C for 2 h, cooled at room temperature and stored in desiccator.

Characterization of different prepared adsorbents

Determination of surface area

The specific surface area (*S*) of the activated carbon was estimated using Sear method (Alzaydian, 2009) by agitating 1.5 g of the adsorbent in 100 ml of diluted hydrochloric acid at a pH of 3. Then, 30 g of NaOH was added while stirring the suspension and the volume was made up to 150 ml with deionized water. The resulting solution was titrated with 0.1 N NaOH to raise the pH from 4 to 9 and the volume, V_{OH}, of NaOH was recorded. The surface area, *S*, of the adsorbent was calculated thus:

$$S = 32V_{OH} - 25 \quad (4)$$

Determination of ash content

The ash content (AC) of the activated carbon was determined by the method of Jeyakumar and Chandrasekaran (2014), and is given by:

$$AC = \frac{M_1}{M \times (100 - X)/100} \times 100 \quad (5)$$

Where, *M* is the mass of sample taken for test, M_1 mass of ash, and *X* the % of moisture content present in sample taken for test.

Determination of bulk density

The apparent or bulk density, ρ_b, of each adsorbent was determined using the tapping procedure described by Ahmeda et al. (1997), and is given by: $\rho_b = W/V_M$, where W is the weight of dry material (g) and V_M the volume of dry material (mL).

Determination of pH

The procedure of Jeyakumar and Chandrasekaran (2014) was used to obtain pH. 10 g of the dried sample was weighed and transferred into a 1 L breaker. 300 mL of freshly boiled water (adjusted to pH 7.0) was added. After digesting for 10 min, the solution was then filtered while hot, rejecting the first 20 mL of the filtrate. The remaining filtrate was then cooled to room temperature and the pH was determined using a pH meter.

Determination of iodine number

The iodine number, *I*, was determined using the method previously described by ASTMD 4607-94 (2006), and is given by:

$$I = \frac{E \times V_B \times c \times 100}{w_s \times 1000} \quad (6)$$

Where, *E* is the equivalent weight of iodine (=127), V_B and *c* the volume and normality of sodium thiosulphate used respectively and w_s the weight of sample used in g.

Fourier-transform infrared (FTIR) analysis

The FTIR analysis of the adsorbents was determined using Shimadzu FTIR-8300 Spectrometer. The corresponding spectra of the chitosan and the derived composite biosorbents were obtained showing the wavelengths in the range 4000 to 400 cm^{-1} of the different functional groups in the samples which were identified by comparison with those in the library.

Preparation of synthetic wastewater

Stock zinc solution of concentration 1000 mg/L was prepared by dissolving 3.93 g of $ZnSO_4.7H_2O$ in 1000 mL of distilled water. The range of initial concentration of the prepared metal solutions varied between 10 and 80 mg/L. The stock solutions were further diluted with distilled water to desired concentrations (test solutions). The pH of the solutions was adjusted with 0.1 N H_2SO_4 and NaOH. Blank experiments were conducted to ensure that no adsorption occurred on the walls of the apparatus used.

Batch adsorption experiment

The batch adsorption studies were carried out at ambient temperature using the different adsorbents prepared: WSC, AWSC, WSCC and AWSCC, for the removal of zinc (II) ions in simulated industrial wastewater at the optimum conditions of all factors that influence adsorption: pH, adsorbent dose, initial metal ion concentration, particle size and agitation time. 30 mg/l of $ZnSO_4.7H_2O$ was prepared by diluting 30 ml of 1000 ml $ZnSO_4$ solution with distilled water in 1000 ml volumetric flask. 100 ml of this aqueous solution was measured into 250 ml Erlenmeyer flasks containing 1 g of each adsorbent. The mixture was mechanically agitated with a basic reciprocating shaker at 150 rpm for 2 h and left undisturbed for 30 min to allow the system to equilibrate. The mixture was filtered, and the concentration of the residual metal ion in the filtrate was determined at $0 \le t \le 180$ min using Atomic Absorption Spectrophotometer (Perkins Elmer Model 3100). The equilibrium metal uptake, q_e (mg/g), adsorption percentage, θ, and adsorption capacity values, q_t (mg/g) at time *t* (min) were calculated using Eqs (7)-(9) respectively:

$$q_e = \left(\frac{c_0 - c_e}{m} \right) V \tag{7}$$

$$\theta = \left(\frac{c_0 - c_e}{c_0} \right) \times 100 \tag{8}$$

$$q_t = \left(\frac{c_0 - c_t}{m} \right) V \tag{9}$$

The distribution ratio, K_d, was determined thus:

$$K_d = \frac{amount\ of\ Zn\ in\ adsorbent}{amount\ of\ Zn\ in\ solution} \times 100 \tag{10}$$

Erdem et al. (2004) correlated the adsorption percentage, θ, and K_d by the following equation:

$$\theta = \frac{100 K_d}{K_d + V/m} \tag{11}$$

All the adsorption experiments were duplicated to ensure accuracy, reliability and reproducibility of the adsorption data. Relative error did not exceed ±0.01.

RESULTS AND DISCUSSION

Fourier Transform Infrared (FTIR) characterization of chitosan

FTIR was performed to confirm the formation of chitosan. The peaks appearing in the FTIR spectrum were assigned to various functional groups according to their respective wave numbers as reported in the literature. Various absorption bands within the 4000-400 cm^{-1} range were recorded in the FTIR spectra of chitosan, prepared from snail shell. The adsorption bands for the prepared chitosan and significant peaks are presented in Table 1.

A characteristic band at 3636.25 and 3348.28 cm^{-1} could be assigned to the stretching vibrations of –NH, -OH, $-NH_2$ and intermolecular hydrogen bonds which overlap each other. The observed peak at 1815.33 cm^{-1} was due to the presence of the methyl group in $NHCOCH_3$. The characteristic –NH band of the prepared chitosan indicates the presence of a carbonyl group at the observed band at 1657.75cm^{-1}, which could be attributed to the incomplete deacetylation of chitin to chitosan. The observed peak at 1087.31cm^{-1} was assigned to –CN stretch of aliphatic amines. The observed band at 941.28 cm^{-1} was indicative of the presence of β-glycolic linkage. The observed band at 856.07 cm^{-1} was attributed to ring stretching and that observed at 710.06 cm^{-1} is attributed to NH out-of-plane bending (Sneha et al., 2014).

The characteristic absorption bands of the prepared chitosan from snail shells were compared with the standard values obtained from Sigma-Aldrich, as shown in Table 2.

Excellent agreements were obtained with AAD being ± 1.10 %, thus confirming the production of chitosan from snail shell used in this study. Also, a straight line was obtained when the experimental data were plotted against the standard data, with a very high coefficient of correlation, $R^2 = 0.9998$ thereby buttressing the earlier statement made.

Determination of degree of deacetylation of chitosan

The degree of deacetylation (*DD*) of chitosan is an important parameter to be noted as it affects the solubility, chemical reactivity and biodegradability of chitosan. *DD* may range from 30% to 95% (Martino et

Table 1. FTIR showing the different bonds present in chitosan.

Wave number (cm^{-1})	Functional groups	Reference
3638.25-3348.25	O–H stretching of the hydroxyl group, N–H stretching	Rumengan et al. (2014)
1815.33	C=O in $NHCOCH_3$ group (amide I band)	Dilyana and Stoyanka (2010)
1657.70	Primary and secondary amide or C=O group	Rumengan et al. (2014)
1388.77	–NO stretch of nitrogen containing compounds and –CO stretch of carbonyl compounds	Dilyana and Stoyanka (2010)
1087.31	–CN stretch of aliphatic amines	Dilyana and Stoyanka (2010)
941.28	β-glycolic linkages	Sneha et al. (2014)
856.07	Ring stretching	Rumengan et al. (2014)
710.06	NH out-of-plane bending	Sneha et al. (2014)

Table 2. Characteristics absorption bands in the FTIR spectra of standard and experimentally prepared chitosan.

Standard wavelength (cm^{-1})	3438	1661	1418	1026	896	752
Experimental wavelength (cm^{-1})	3348.25	1657.70	1388.77	1028.31	885.07	750.06
% error	±2.61	±0.20	±2.06	±0.23	±1.22	±0.26

Table 3. Proximate analyses of chitin and chitosan from snail shell.

Materials	Proximate analysis, %			
	Moisture content	Ash content	Protein	Fibre
Chitin	9.00	3.80	10.40	4.09
Chitosan	5.20	6.39	6.14	8.72

al., 2005), depending on the available source and procedure. 100% *DD* is very scarcely obtained, with commercial chitosan with various *DD* in the range of 75-85%. IR technique was used for determining the degree of deacetylation, *DD*, of chitosan, according to the methods described by Domszy and Roberts (1985) and Hiral et al. (1991) using Equation (12):

$$DD = 100\left(1 - \frac{A_{1657.70}}{A_{334825}} \times \frac{1}{1.33}\right) \quad (12)$$

Where, $A_{1657.70}$ and A_{334925} are values of absorbance at the wavelengths 1657.70 and 3349.25 cm^{-1} respectively. From the FTIR analysis of chitosan, the % transmittance of the wavelength 1657.70 and 3349.25 cm^{-1} was obtained as 95 and 78 respectively. This was then converted to absorbance [=2-log (% transmittance)] to determine the degree of deacetylation of the prepared chitosan from snail shells as 85.53%, using Equation 12. This value is in the range given by Martino et al. (2005).

Proximate analysis of chitin and chitosan

The proximate analyses of chitin and chitosan prepared in this study are presented in Table 3.

It was found that the moisture content of chitin was higher than that of chitosan owing to the fact that water was removed from the chitin prior to the production of chitosan. The ash content of chitin was lower than that of chitosan as a result of the presence of the acetyl group in the chitin sample. Protein content of the chitin was high after deproteinization of the chitin and this could be attributed to the low degree of acetylation of the chitin, which was found to be 14.47% (that is 100-DD of chitosan). The fibre content of the chitosan was higher than that of chitin owing to the fact that the removal of more matter from the chitin to obtain chitosan could have

Table 4. Ultimate and proximate analyses of raw walnut shell.

Ultimate analysis (%)					Proximate analysis (%)			
C	H	N	S	O	Moisture content	Ash content	Volatile matter	Fixed carbon
45.90	5.90	0.25	0.00	47.95	11.60	1.40	70.50	16.50

Table 5. Proximate analysis and physicochemical properties of the prepared adsorbents.

Proximate analysis	Adsorbents			
	WSC	AWSC	WSCC	AWSCC
Moisture content (%)	6.72	5.10	5.56	4.78
Ash content (%)	6.50	1.49	5.60	2.60
Volatile matter (%)	10.56	9.28	8.76	7.54
Fixed carbon (%)	17.08	16.54	17.20	16.71
Physicochemical properties				
Surface area (m^2/g)	620	634	650	890
Bulk density (g/ml)	0.30	0.50	0.40	0.60
pH	9.0	7.6	9.0	5.5
Iodine value (mg/g)	135	168	200	172

led to the presence of more fibre in the chitosan than in chitin. The results of the proximate analysis of chitin and chitosan obtained in this study were consistent with those obtained by Isa et al. (2012) in the extraction and characterization of chitin and chitosan from Nigerian shrimps.

The solubility of chitosan was checked using four different solvents: water, ethanol, NaOH and ethanoic acid. It was found that the chitosan was soluble in acidic condition but insoluble in alkaline, ethanol and neutral solution. The pH value of the chitosan also varied from 6.3 to 8.2, as reported by Sneha et al. (2014) in the extraction and purification of chitosan from chitin isolated from sea prawn.

Ultimate and proximate analyses of raw walnut shell

The results of the ultimate and proximate analyses of the walnut shell are given in Table 4.

From the ultimate analysis, the precursor for the preparation of different adsorbents used in this study has very low nitrogen and no sulphur and thus cannot contribute to environmental issues involving oxides of nitrogen and sulphur. Also, the walnut shells have a high volatile matter content and low ash content, which is essential for pyrolysis and gasification processes.

The lignocellulosic composition of the walnut shell was determined according to the Robertson and Van Soest (1981) method. The % of cellulose, hemicellulose and lignin was found to be 41.40, 20.00 and 17.60 respectively. Thus, the lignin content of the walnut shell used in this study was least. However, materials with a low content of the lignin fraction are candidates for the production of microporous activated carbon (Daud and Ali, 2004; Gergova et al., 1994).

Characteristics of the prepared adsorbents

Table 5 shows the characteristics of the prepared adsorbents. The moisture content of AWSCC was 4.78%, which was the lowest amongst the prepared adsorbents. Hence, AWSCC could be adjudged the best adsorbent amongst the prepared adsorbents, with excellent adsorption performance since lower moisture content increases the adsorption capacity of carbon by concentrating the action of activated carbon.

The ash content of AWSCC was found to be 2.60%, which was the lowest amongst the investigated adsorbents. The lower the ash content, the better the starting material for removal of heavy metal ions from industrial wastewater (Lin and Wu, 2001). Hence, AWSCC was found to be a better adsorbent than WSC, AWSC and WSCC. Moreover, the least ash content value for AWSCC was favourable because the ash content can interfere with the adsorption process (Khan et al., 2009).

AWSCC has the lowest volatile matter compared to WSC, AWSC and WSCC. This can be attributed to the fact that during thermal activation, most of the non-carbon elements such as hydrogen, oxygen, nitrogen and sulphur might have been eliminated as volatile gaseous products by the pyrolysis.

There is no much difference on the fixed carbon content of WSC, AWSC, WSCC and AWSCC, as the % error between the highest and lowest values for WSCC and AWSC respectively was ±3.84<±5.. Hence, all the prepared adsorbents in this study could be viable options for activated carbon production.

The surface area of an activated carbon is directly related to the porosity of the carbon. From Table 5, the increasing order of surface areas of the prepared adsorbents was WSC < WSCC < AWSC < AWSCC. Therefore, AWSCC could be adjudged the best and highly porous adsorbent. However, the surface areas of these adsorbents conformed to the range for plant adsorbents, which is between 10^2 and 10^3 m^2/g.

The results of bulk density of the prepared adsorbents revealed that AWSCC had the highest bulk density, which is indicative of higher quality adsorbent than the other three adsorbents. Therefore, AWSCC could provide better contact with the adsorbate, leading to more effective adsorption process.

The pH parameter is a factor affecting adsorption capacity of heavy metals. It is well known that pH could affect the protonation of functional group on the active sites of the adsorbent, as well as metal chemistry (Tsezos and Bell, 1989). The pH values of WSC, AWSC, WSCC and AWSCC were determined to be 9.0, 7.6, 9.0 and 5.5. These findings were in agreement Cheremisnoff and Ellerbusch (1978) who confirmed that the pH of either raw or carbonized agricultural materials in water suspension can vary between 4 and 12.

Iodine value is a fundamental parameter used to characterize the performance of activated carbons. It is often used to determine the micropore content of the activated carbon and is obtained by the adsorption of iodine from solution by the activated carbon sample (Jeyakumar and Chandrasekaran, 2014). Higher value of the iodine value indicates higher degree of activation. The iodine values of WSC, AWSC, WSCC and AWSCC are given in Table 5. The WSCC had the highest iodine value of 200 mg/g, indicating that its pore surface and structure were the best developed in this study.

Fourier Transform Infrared (FTIR) characterization of prepared adsorbents

The FTIR spectra of the prepared biosorbents were studied in the range of 4000 to 400 cm^{-1}. The FTIR spectra of the WSC and AWSC obtained in this study did not exhibit significant differences in the surface chemistry of these two adsorbents. However, slight differences on the intensity of the bands were detected. The following surface functional groups were identified for WSC and AWSC (González et al., 2009). The wide bands at 3400 cm^{-1} were related to vibrations *v*(O–H) in water molecules. The weak band was found around 2900 cm^{-1}, which was attributed to carboxylic acids or aliphatic groups. The band at 2350 cm^{-1} is generally associated with vibrations in aliphatic bonds. The bands within the region 1400-1800 cm^{-1} can be attributed to C=O bonds, which is related to the presence of carbonyl groups or aromatic rings. Finally, the weak band detected around 1123 cm^{-1} was related to *v*(C–O) bonds in lactones, epoxides and ether structures.

For WSCC, the broad band positioned between 3375.99 and 3334.25 cm^{-1} revealed the existence of –OH stretching of the hydroxyl group, intra molecular hydrogen groups and free N–H. The observed band at 2943.90 and 2360.41 cm^{-1} was attributed to C–H stretching. The observed band at 2193.00 and 1977.95 cm^{-1} was as a result –C ≡ C– (alkyne). The observed band at 1617.55 cm^{-1} could be attributed to primary and secondary amide or C=O group present in WSCC. The observed band at 1503.37 cm^{-1} was as a result of N–H deforming. The observed band at 1459.90 cm^{-1} was attributed C–C stretch (in ring). The observed band at 1374.62 cm^{-1} was indicative of CH_3 in the $NHCOCH_3$ group. The observed band at 1317.77 and 1264.49 cm^{-1} was due to nitrate (NO_2) symmetric stretching vibration. The observed band at 1029.05 cm^{-1} was as a result of the stretching of the CO bond. The observed band at 886.37 cm^{-1} was indicative of the stretching of O-O bond and the observed band at 813.95-661.81 cm^{-1} was as a result of the stretching of halogenated compounds, C–X, where 'X' represents halogens.

For AWSCC, the broad band positioned at 3431 cm^{-1} revealed the existence of –OH stretching of the hydroxyl group. The 1615.80 cm^{-1} band was a bend vibration of N–H (Argun and Dursun, 2006). The observed band at 1315.80 cm^{-1} was as a result of the nitrate (NO_2) symmetric stretching vibration and the observed band at 1056.60 cm^{-1} was attributed to the vibration C=O=C and O–H in polysaccharides. The observed band at 879.73 cm^{-1} was due to the $C=CH_2$ bending and that at 779.26 and 659.06 cm^{-1} could be attributed to the presence of the SO_3 group and C–S stretching respectively.

Dynamics of Zn II ions adsorption on prepared adsorbents

Effect of pH on the removal of Zn (II) ions

While operational parameters (adsorbent dose, agitation time and initial metal ion concentration) were kept constant and temperature and agitation speed kept at 30°C and 150 rpm respectively, the results of the effect of solution pH (2≤pH≤9) on the adsorption of Zn (II) ions onto WSC, AWSC, WSCC and AWSCC are shown in Figure 1. It was observed that the adsorption capacities of WSC, AWSC, WSCC and AWSCC for Zn (II) ions removal increased as pH increased until optimum pH value of 5, and then decreased when pH was increased further. This may be due to the formation of soluble

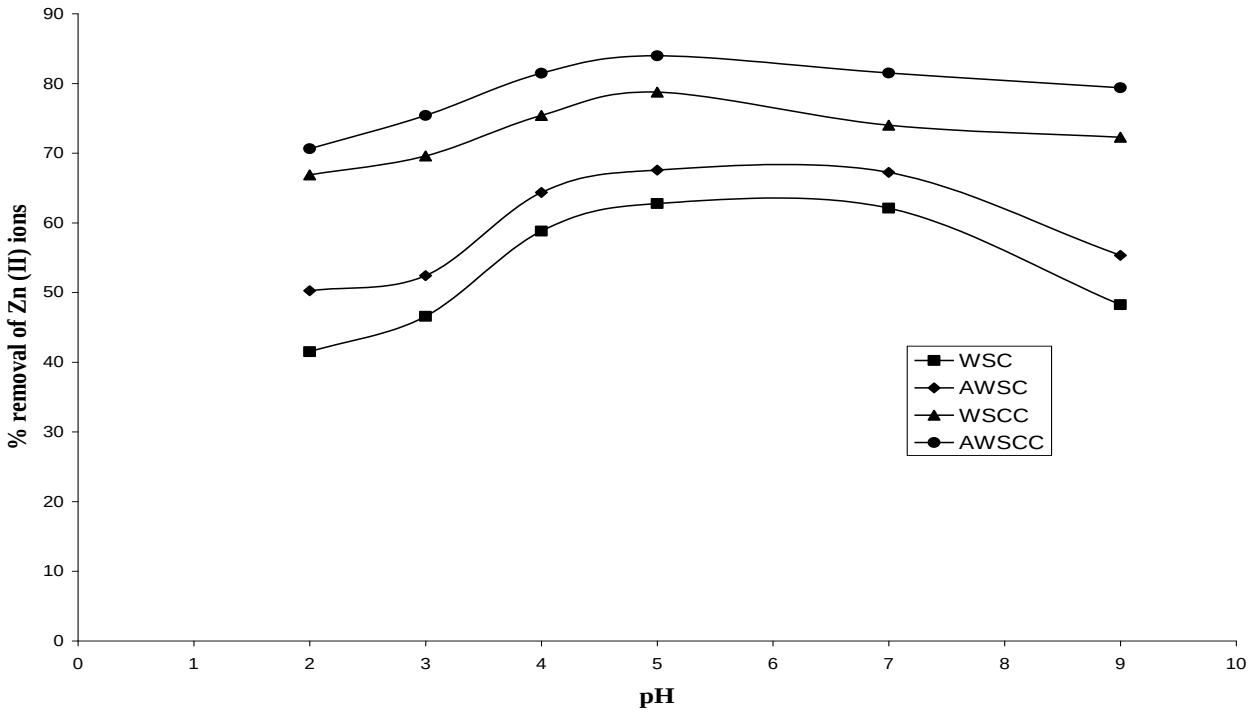

Figure 1. Effect of pH on the removal efficiency of Zn (II) ions using WSC, AWSC, WSCC and AWSCC at $c_0 = 30$ mg/L, dose of each adsorbent=1g, agitation speed=150 rpm, contact time=120 min, particle size=60BSS and temperature of solution=30°C.

hydroxyl complexes. The onset of metal hydrolysis and precipitation begins at pH > 5 (Baes and Mesmer, 1976). Competitive adsorptions between H^+ and Zn^{2+} ions result in low adsorption efficiency of Zn^{2+} as H^+ concentration increases if pH is below 3 (Amuda et al., 2007). At low pH, the amine group on the chitosan is protonated to a varying degree (Nomanbhay and Palanisamy, 2005). The surface acidity was due to the introduction of several oxygen-containing functional groups (Faria et al., 2004). Acid activation of walnut shell carbon using phosphoric acid and subsequent impregnation on chitosan to produce AWSCC improved the electrostatic interaction between chitosan and AWSC. Hence, more active sites were available for the adsorption of Zn (II) ions on AWSCC thereby resulting in the highest metal ion removal efficiency as shown in Figure 1. Therefore, the increasing order of Zn (II) ions removal efficiency at pH between 2 and 9 is WSC<AWSC<WSCC<AWSCC.

Effect of adsorbent dosage on the removal of Zn (II) ions

Figure 2 shows Zn (II) ions removal efficiency as function of adsorbents dosage. The dose of each adsorbent was varied between 5 and 25 g/L, keeping other operational parameters (pH, agitation time, initial ion concentration and particle size) at the optimum and temperature and agitation speed were kept at 30°C and 150 rpm respectively. Owing to the availability of more binding sites, it was observed that increasing the dose of the each adsorbent increased the removal efficiency of Zn (II) ions. However, increasing the dose of the adsorbents above 15 g/L for WSC, 20 g/L for AWSC, 15 g/L for WSCC and 10 g/L for AWSCC produced no appreciable increase in the Zn (II) ions removal efficiency. The highest Zn (II) removal efficiency for WSC and AWSC was 65.64 and 71.67% respectively at 25 g/L dose of the adsorbent. As it can be seen from Figure 2, 15 g/L and 10 g/L dose of WSCC and AWSCCC respectively exhibited 79.76 and 83.81% Zn (II) ions removal efficiency respectively, indicating that surface area of the carbon has significant effect on the removal of Zn (II) from synthetic wastewater. In Table 5, AWSCC had the highest surface area thereby the highest Zn (II) ions removal efficiency. Therefore, the decreasing order of the surface area and thus Zn (II) ions removal efficiency is AWSCC>WSCC>AWSC>WSC. From Figure 2, it can be seen that after a certain dose of adsorbent, no significant amount of ions is bound to the adsorbent. The amount of free ions remains constant even with further addition of the dose of adsorbent (Nomanbhay and Palanisamy, 2005). The difference in the surface

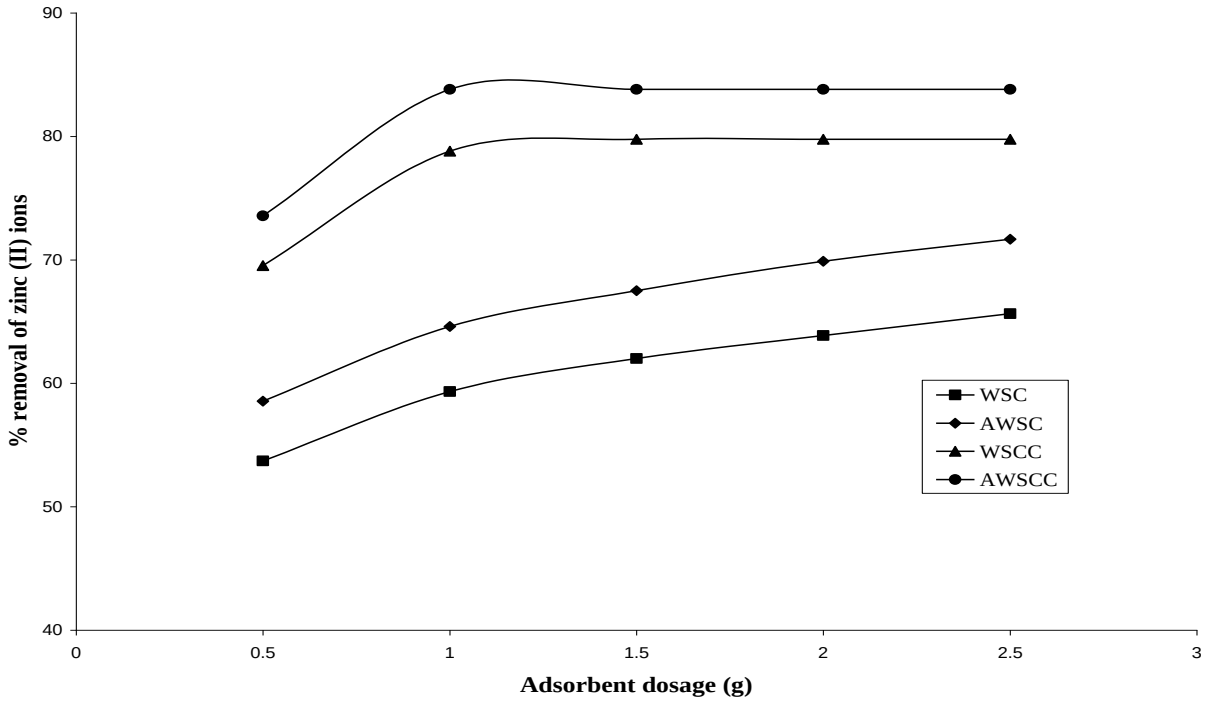

Figure 2. Effect of adsorbent dosage on the removal efficiency of Zn (II) ions using WSC, AWSC, WSCC and AWSCC at $c_0 = 30$ mg/L, pH=5, agitation speed=150 rpm, contact time=120 min, particle size=60BSS and temperature of solution=30^{o}C.

modification of the adsorbents conferred on them different degrees of removal efficiency. The oxidation of WSC with mineral acids has been implicated to introduce more acidic C=O groups on the surface of WSC. This would enhance the electrostatic interaction between chitosan and the more negatively charged AWSCC, thus, preventing agglomeration of chitosan (Amuda et al., 2007). The formation of more acidic surface oxides on AWSCC than WSC, AWSC and WSCC enhanced efficient coating of chitosan, enhanced its hydrophilic character and hence improved the hydrodynamic flow of metal ion to the acidic surface oxides on the carbon surface. This could be responsible for the high adsorption capacity of AWSCC over WSC, AWSC and WSCC.

Effect of initial metal ion concentration on the removal of Zn (II) ions

The percentage removal of Zn (II) ions by the adsorbents initially increased rapidly with increasing Zn (II) ions concentration and stagnates when Zn (II) concentration reached 30mg/L, as can be seen in Figure 3. At lower concentrations, Zn (II) ions in the solution would interact with the binding sites and thus facilitated 100% adsorption (Amuda et al., 2007). At higher concentrations, more Zn (II) ions were left unadsorbed in solution due to the saturation of binding sites, which was indicative of the involvement of energetically less favourable sites with increasing metal ion concentrations in the aqueous solution. The Zn (II) ion adsorption could be attributed to different mechanisms of ion exchange processes as well as to the adsorption process. During the ion exchange process, Zn (II) ions had to move through the pores of the adsorbent mass, as well as through channels of the lattice, thereby replacing exchangeable cations. Diffusion was rapid through the pores and was retarded when the ions moved through the smaller diameter channels. In this case, the Zn (II) ions sorption could mainly be attributed to ion-exchange reactions in the micropores of the adsorbents (Amuda et al., 2007). The maximum percentage of Zn (II) ions removal of 52.2 and 55.1 was achieved when 75 mg/L Zn (II) ion concentrations was adsorbed with 1 g/100 mL of WSC and AWSC while the maximum percentage of Zn (II) ions removal of 95.4 and 97.8 was achieved when 50 mg/L Zn (II) ion concentrations was adsorbed with 1 g/100 mL of WSCC and AWSCC.

Effect of contact time on the removal of Zn (II) ions

Equilibrium time is another important operational

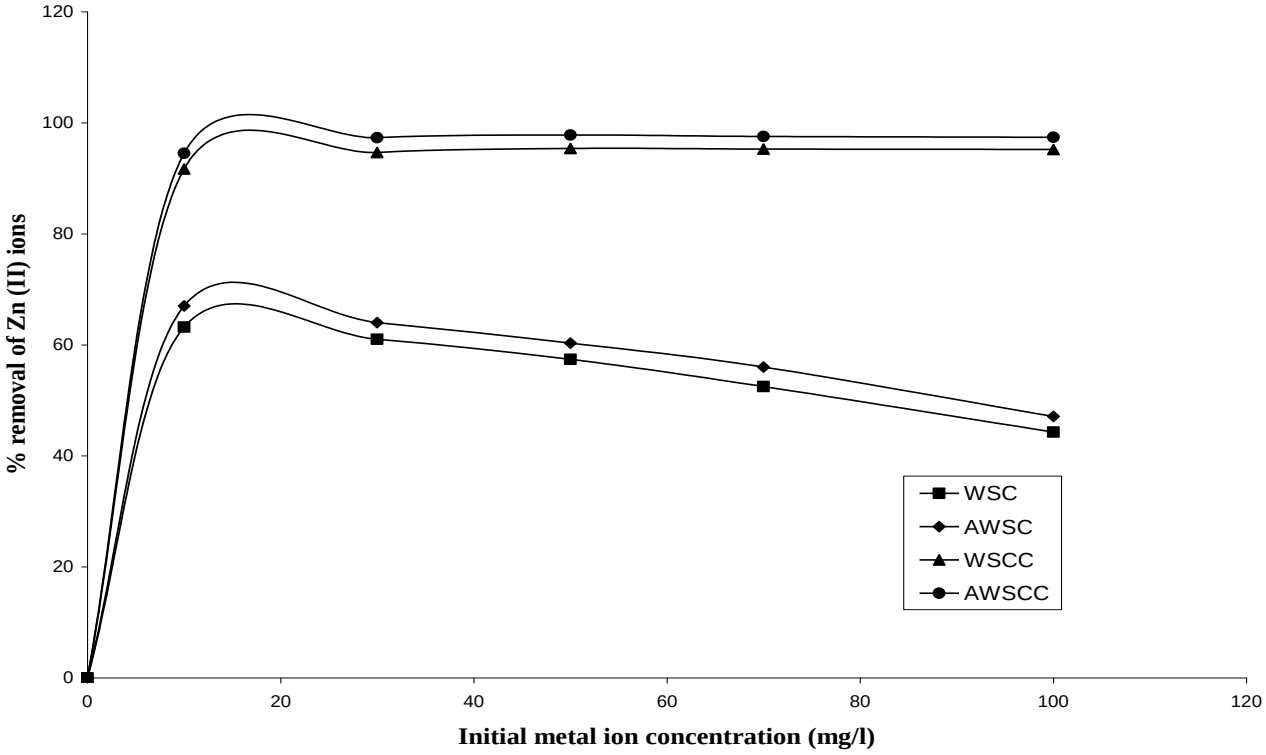

Figure 3. Effect of initial metal ion concentration on the removal efficiency of Zn (II) ions using WSC, AWSC, WSCC and AWSCC at pH=5, dose of each adsorbent=1 g, agitation speed=150 rpm, contact time=120 min, particle size=60BSS and temperature of solution=30^{o}C.

parameter for an economical wastewater treatment process. Figure 4 depicts Zn (II) ions removal efficiency as function of agitation time keeping pH and adsorbent dose at the optimum and temperature and agitation speed at 30°C and 150 rpm, respectively. From the Figure, increase in agitation time increased the removal efficiency of Zn (II) ions until equilibrium adsorption was established. Equilibrium adsorptions were established within 180 min for WSC, AWSC, WSCC and AWSCC with Zn (II) ions removal efficiencies of 62.5%, 68%, 81.8% and 85.4% respectively. This was due to greater availability of various functional groups on the surface of chitosan required for interaction with anions and cations and thus significantly improved the binding capacity and the process proceeded rapidly for AWSCC and WSCC, compared to WSC and AWSC.

Effect of agitation speed on the removal of Zn (II) ions

Figure 5 shows the effect of agitation speed on the percentage removal of Zn (II) ions from industrial wastewater using WSC, AWSC, WSCC and AWSCC as adsorbents, while other parameters such as pH and adsorbents dose were kept at the optimum and temperature at 30°C. It can be seen that the removal efficiency of Zn (II) ions using the four prepared adsorbents increased as the agitation speed increased until the optimum value and then decreased when the agitation speed further increased. This can be attributed to the fact that an increase in the agitation speed led to improvement in the mixing between metal ions in solution and active binding sites of the adsorbents (WSC, AWSC, WSCC and AWSCC) thereby resulting in an increased removal efficiency of Zn (II) ions. When the mixture of metal ion and the adsorbents (WSC, AWSC, WSCC and AWSCC) was set on a shaker in several Erlenmeyer flasks, the fine particles of WSC, AWSC, WSCC and AWSCC moved rapidly in the metal solution and this led to increased concentration of metal ions near the surface of the active sites. According to Kafia and Surchi (2011), the high shaking speed provided sufficient additional energy to break newly formed weak bonds between the metal ions and binding sites of the adsorbent. Consequently, high agitation speed may lead to the adsorbed metal ions to desorb from the adsorption sites. From Figure 5, at the optimum agitation speed of 150 rpm, the respective value of the removal efficiency of Zn (II) ions was found to be 60.3, 64.1, 82 and 85.4% using WSC, AWSC, WSCC and AWSCC as adsorbents

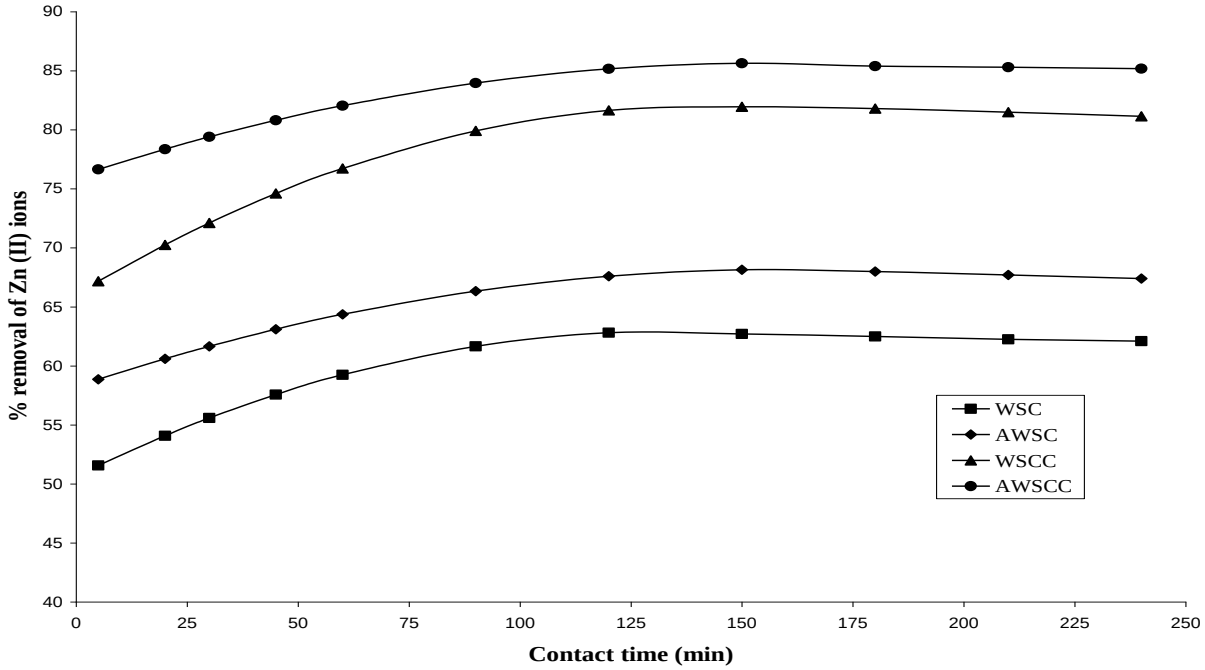

Figure 4. Effect of contact time on the removal efficiency of Zn (II) ions using WSC, AWSC, WSCC and AWSCC at $c_0 = 50$ mg/L, pH=5, dose of each adsorbent=1 g, agitation speed=150 rpm, contact time=120 min, particle size=60BSS and temperature of solution=30°C.

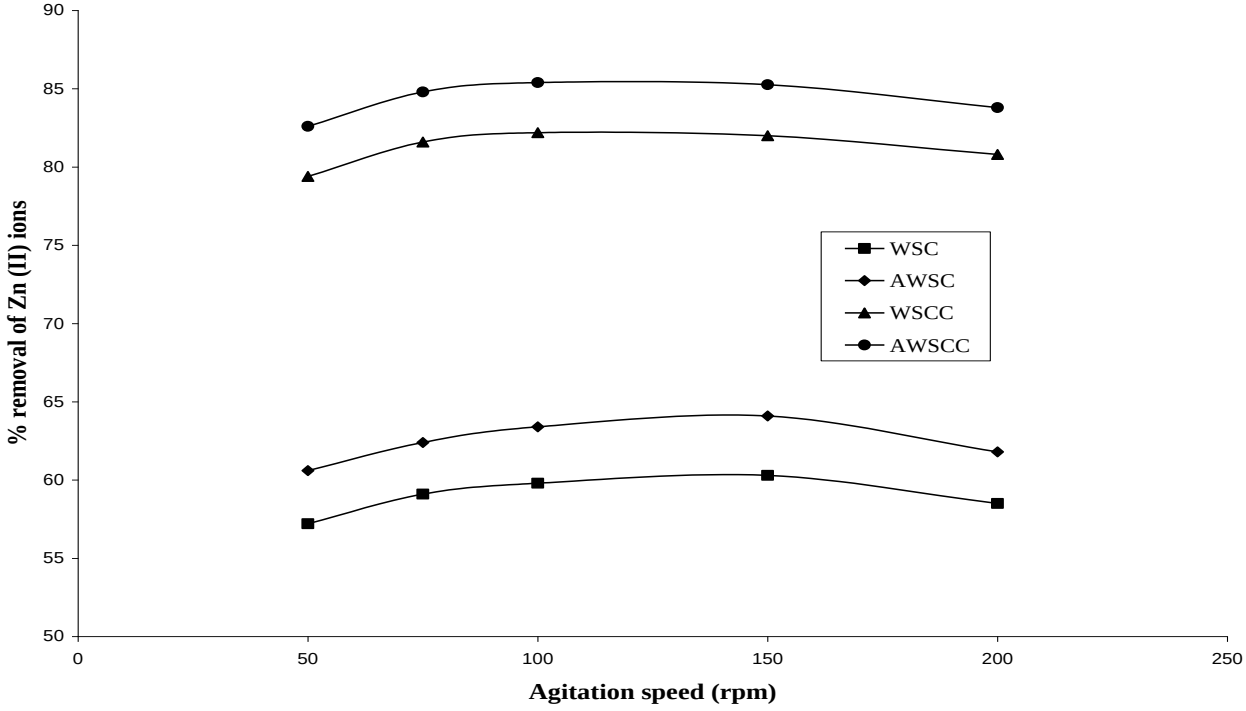

Figure 5. Effect of agitation speed on the removal efficiency of Zn (II) ions using WSC, AWSC, WSCC and AWSCC at $c_0 = 50$ mg/L, dose of each adsorbent=1g, agitation speed=150 rpm, contact time=120 min, particle size=60BSS and temperature of solution=30°C.

thereby giving justification to setting agitation speed to 150 rpm for all adsorption studied in this work.

Correlation of equilibrium adsorption data

The sorption equilibrium data gathered in this study were confronted with the adsorption isotherms of Langmuir, Freundlich and Temkin. These isotherms are given as follows:

Langmuir isotherm: $$q_e = \frac{q_{\max} K_L c_e}{1 + K_L c_e} \quad (13)$$

Which can be linearized to five different linear forms:

$$\frac{1}{q_e} = \frac{1}{K_L q_{\max}} \frac{1}{c_e} + \frac{1}{q_{\max}}, \quad \frac{c_e}{q_e} = \frac{1}{q_{\max}} c_e + \frac{1}{K_L q_{\max}}$$

$$q_e = \frac{1}{K_L} \frac{q_e}{c_e} + q_{\max}, \quad \frac{q_e}{c_e} = -K_L q_e + K_L q_{\max}, \quad \text{and}$$

$$\frac{1}{c_e} = -K_L q_{\max} \frac{1}{q_e} - K_L$$

The important characteristics of Langmiur isotherm was explained by a dimensionless constant, known as separation factor or equilibrium parameter, R_L, given by Zhai et al. (2004):

$$R_L = \frac{1}{1 + K_L c_0} \quad (14)$$

Using mathematical computations, Zhai et al. (2004) showed that R_L indicates the shape of the isotherm thus: for $R_L < 0$, $0 < R_L < 1$, $R_L = 1$ and $R_L > 1$, we have irreversible, favourable, linear and unfavourable isotherms respectively.

Freundlich isotherm: $$q_e = K_F c_e^{1/n} \quad (15)$$

Whose linear form is expressed thus:

$$In\, q_e = In\, K_F + \frac{1}{n} In\, c_e \quad (16)$$

Where, K_F is a measure of adsorption capacity and *n* stands for the heterogeneity.

Temkin isotherm: $$q_e = \frac{RT}{b_T} In(A_T c_e) = \frac{RT}{b_T}(In\, A_T + In\, c_e) \quad (17)$$

In these isotherms, necessary linear plots were made, as shown in Figures 6 to 8, slope and intercept were determined and the inherent isotherm parameters were calculated as shown in Tables 6 and 7.

The coefficient of correlation, R^2, was the criterion for fitting the experimental data to these isotherms. It should be stressed that all the five linearized forms of Langmuir isotherm were fitted to the experimental data, and they all gave almost the same results. From the R^2 values, Langmuir isotherm correlated exceedingly well the equilibrium adsorption data of Zn^{2+} ions removal using WSC, AWSC, WSCC and AWSCC as adsorbents. The maximum uptake capacities for Zn^{2+} ions were 17.70, 16.45, 3.80 and 3.11 mg/g for AWSCC, WSCC, AWSC and WSC respectively. The Langmuir parameters were also used to predict the affinity of the adsorbents' surfaces toward the Zn^{2+} ions by using dimensionless separation factor, R_L, as expressed in Equation 12. The R_L values obtained were in the range $0 < R_L < 1$ for Zn^{2+} ions concentration studied in this work ($20 < c_O < 200$ mg/l). This is indicative of a favourable isotherm shape for the adsorption of Zn^{2+} ions onto WSC, AWSC, WSCC and AWSCC in the concentration range studied.

Though n>1 for the four adsorbents using Freundlich isotherm, the R^2 value for AWSC is not that close to unity while promising results were obtained for WSC, WSCC and AWSCC. The *n* value of Freundlich equation gives an indication of the favourability of sorption. It is generally stated that values of *n* in the range of 2 to 10 are good, 1 to 2 as moderately difficult and less than 1 as poor sorption characteristic (Chen et al., 2010). Hence, Freundlich isotherm can be used to correlate the adsorption data of Zn^{2+} ions removal using WSC, WSCC and AWSCC as adsorbents, with the best fitted adsorption data obtained for AWSCC.

The estimated values of Temkin parameters and R^2 are presented in Table 7. From the R^2 values, which are close to unity, Temkin isotherm could also be a representative for the Zn^{2+} ions adsorption onto the four adsorbents studied.

In general, Langmuir adsorption isotherm had the best fit for the four adsorbents tested in this study as a result of the highest correlation coefficient. The suitability and applicability of Langmuir isotherm to the adsorption of Zn^{2+} ions on WSC, AWSC, WSCC, and AWSCC reveal the formation of monolayer coverage of the Zn^{2+} ions on the surface of these adsorbents.

Kinetic modelling of Zn (II) ions adsorption

Different kinetic models given in Equations 18, 20, 23, 24 and 26 were used to test the kinetic data for the adsorption of Zn^{2+} ions on WSC, AWSC, WSCC and AWSCC.

The fractional power model, which has the form of

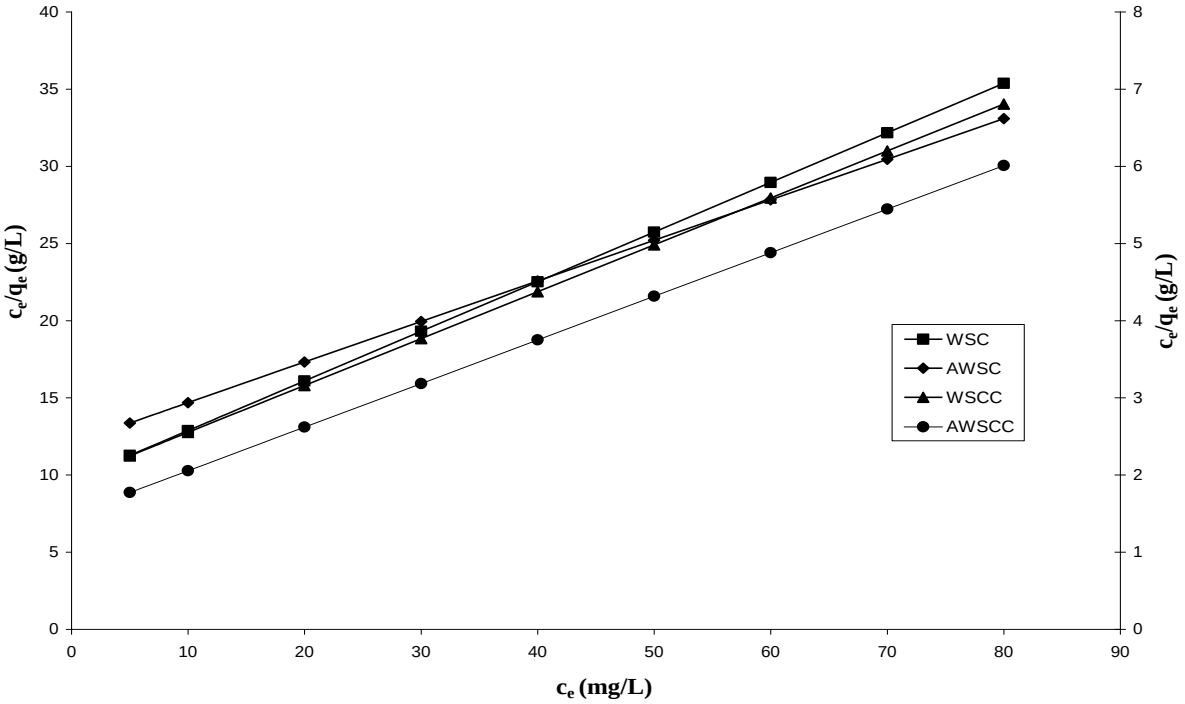

Figure 6. Langmuir adsorption isotherm fitted to the batch equilibrium data of Zn (II) ions adsorption on WSC, AWSC, WSCC and AWSCC as adsorbents.

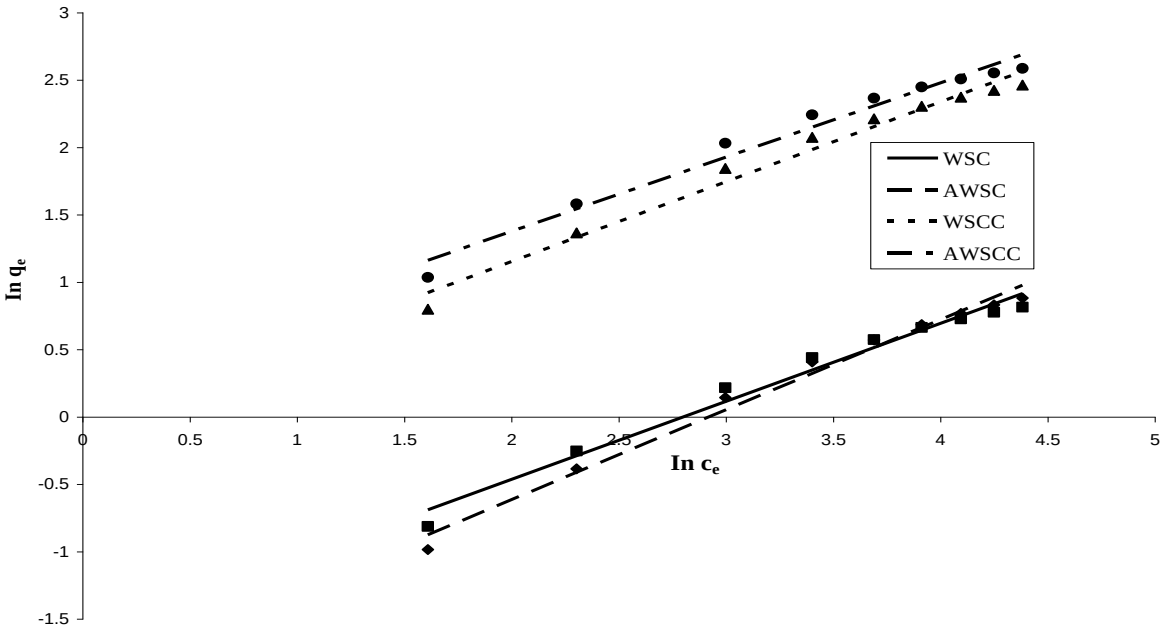

Figure 7. Freundlich adsorption isotherm fitted to the batch equilibrium data of Zn (II) ions adsorption on WSC, AWSC, WSCC and AWSCC as adsorbents.

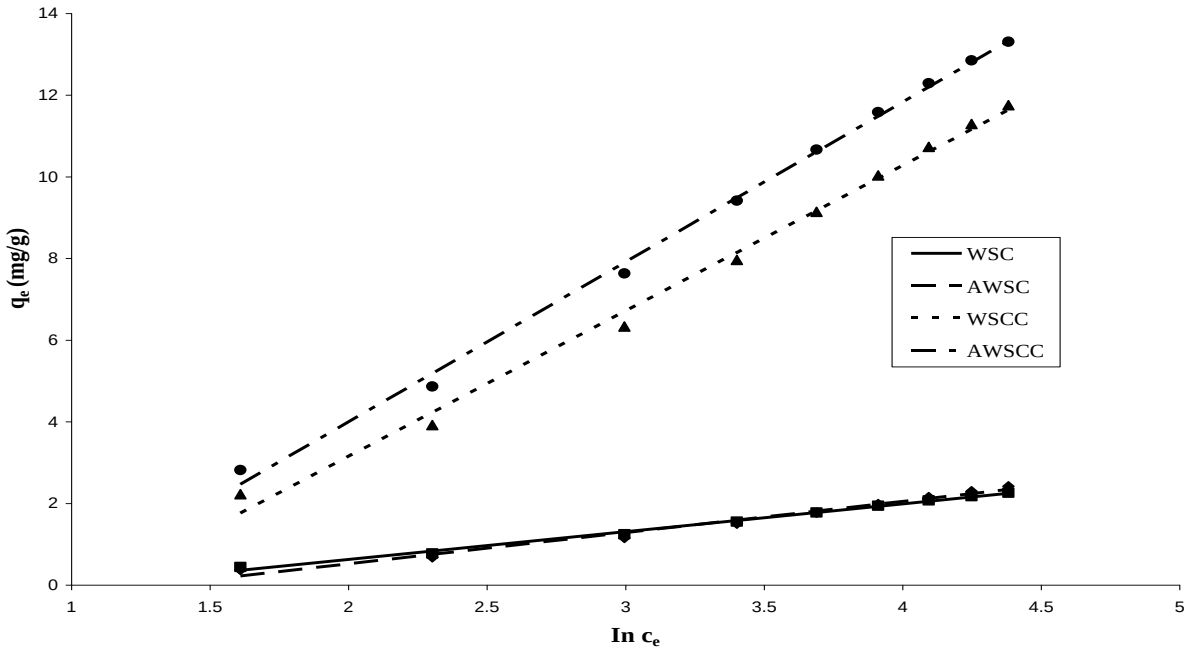

Figure 8. Temkin isotherm fitted to the batch equilibrium data of Zn (II) ions adsorption on WSC, AWSC, WSCC and AWSCC as adsorbents.

Table 6. Langmuir and Freundlich isotherm parameters for adsorption of Zn^{2+} ions by different adsorbents at 30°C.

Adsorbent	Langmuir parameters				Freundlich parameters		
	q_{max} (mg/g)	K_L (L/mg)	R_L	R^2	K_F (mg/g)	*n*	R^2
WSC	3.1104	0.0333	0.6002	0.9997	2.224	2.9586	0.941
AWSC	3.8052	0.0218	0.6964	0.9998	2.808	2.1505	0.918
WSCC	16.4474	0.0313	0.6150	0.9997	1.0392	1.5952	0.9701
AWSCC	17.6991	0.0379	0.5688	1.0	0.8690	1.6036	0.9754

Table 7. Temkin isotherm parameters for adsorption of Zn^{2+} ions by different adsorbents at 30°C.

Adsorbent	Temkin parameters			
	A_T (L/g)	b_T	$\Phi_1 (= RT/b_T)$	R^2
WSC	0.3422	3710.08	0.6790	0.9753
AWSC	0.2678	3297.74	0.7639	0.9848
WSCC	3.2845	802.63	3.0868	0.9813
AWSCC	3.5570	693.53	2.6950	0.9885

Freundlich equation, indicates the metal uptake increases exponentially with time, and is given by:

$$q_t = k_F t^N \quad (18)$$

Taking natural logarithms of Eq. (16) gives:

$$In\, q_t = In\, k_F + N\, In\, t \quad (19)$$

Hence, the parameters inherent in the model can be estimated by making appropriate linear plot of $In\, q_t$ against $In\, t$

The Elovich kinetic model is given by:

$$\frac{dq_t}{dt} = \alpha \exp(-\beta q_t) \quad (20)$$

Where, α and β are constants during an experiment. As $q_t \to 0,\ dq_t/dt \to \alpha$, hence α is regarded as the initial rate of adsorption. When $t=0,\ q_t=0$ and $t=t,\ q_t=q_t$, the integrated form of Equation 20 is:

$$q_t = \frac{1}{\beta}\left[In(t+\Phi) - In\,\Phi\right] \quad (21)$$

Where, $\Phi = 1/(\alpha\beta)$. If $t >> \Phi$, Eq. (21) simplifies to:

$$q_t = \frac{1}{\beta} In(\alpha\beta) + \frac{1}{\beta} In\,t \quad (22)$$

Hence, a linear plot of q_t against *In t* can be made to check if $t >> \Phi$ for the coefficient of determination, R^2, should be greater than 1.

The intraparticle diffusion (IPD) (or Weber and Morris) model is used to identify the mechanism involved in the adsorption process. IPD model has the form:

$$q_t = k_{IPD}\sqrt{t} \quad (23)$$

A linear plot of q_t against $\sqrt{t}$ can be used to determine k_{IPD}, with no intercept on q_t axis.

The Lagergren pseudo first-order kinetic model is expressed as:

$$\frac{dq_t}{dt} = k_1(q_e - q_t) \quad (24)$$

The integrated form of Equation (24) is:

$$In(q_e - q_t) = In\,q_e - k_1 t \quad (25)$$

The specific reaction rate constant, k_1, for the Lagergren pseudo first-order kinetics is usually obtained by plotting $In(q_e - q_t)$ against t, whereby the slope of the straight line obtained is $-k_1$.

The pseudo second-order kinetic model is given by:

$$\frac{dq_t}{dt} = k_2(q_e - q_t)^2 \quad (26)$$

The integrated form of equation (26) is:

$$q_t = \frac{k_2 q_e^2 t}{1 + k_2 q_e t} \quad (27)$$

Which gives different forms when linearized. One of such forms used in this study is:

$$\frac{t}{q_t} = \frac{1}{k_2 q_e^2} + \frac{t}{q_e} \quad (28)$$

Hence, a plot of t/q_t against *t* should yield a straight line to enable the determination of q_e and k_2 from slope and intercept respectively.

The goodness of fit was justified based on the fact that the coefficients of determination were close to 1. The models, their estimated parameters and R^2 values are presented in Table 8.

Though the value of the exponent, *N*, of the fractional power model was less than 1, which indicated the time-dependent of the adsorption of Zn^{2+} ions on WSC, AWSC, WSCC and AWSCC as adsorbents, the fractional power model did not provide a good fit to the kinetic data of the adsorption of Zn^{2+} ions as the coefficients of correlation, R^2, in all cases of the four adsorbents used in this study, were not close to unity, as presented in Table 8. Moreover, the experimental kinetic data did not show satisfactory fit to Elovich kinetic model since R^2 values for the four adsorbents used were not close to unity. The kinetic plots for the intraparticle diffusion model obtained in this study for the four adsorbents tested were not linear for all the lines did not pass through the origin as expected: they all had intercepts, *C*, as shown in Table 8. This indicated that the intraparticle diffusion was not the rate-controlling step in the adsorption of Zn^{2+} ions on the prepared adsorbents, and there was some degree of boundary layer diffusion. This was buttressed by the fact that the correlation coefficients are far less than unity. In fact, in all the kinetic models studied, IPD shows the worst fit of the kinetic data. Also, Table 8 depicts the kinetic parameters and the R^2 values for the Lagergren's pseudo first-order kinetic model and the pseudo second-order kinetic model. Although the R^2 values were somewhat high for the former, its theoretical values of q_e in Table 8 were far less than the corresponding experimental values predicted by the latter. This suggested a poor fit between the kinetics data and the Lagergren pseudo-first order kinetic model for the four adsorbents used in this study. These results were in consonance with similar works in the literature (Lodi et al., 1998; Ho and Mckay, 2000) with several natural adsorbents and the same initial concentration values. Excellent agreements were obtained between the

Table 8. Kinetic model parameter values and coefficient of correlation values.

Kinetic model	Parameter values	Adsorbents			
		WSC	AWSC	WSCC	AWSCC
Fractional power law	k_F	2.7665	3.2904	2.5118	3.3814
	N	0.0538	0.0367	0.0844	0.0404
	R^2	0.8368	0.8308	0.8486	0.8321
Elovich model	α (mg/g min)	238671.10	1.07×10^{9}	286.47	9.76×10^{7}
	β (g/mg)	5.2493	7.0126	2.9931	6.0827
	R^2	0.8551	0.8435	0.8772	0.8461
IPD model	k_{IPD} (mg/g min^{½})	0.0247	0.0184	0.0437	0.0213
	C (mg/g)	3.2922	3.7059	3.3343	3.8551
	R^2	0.6715	0.6572	0.6997	0.6604
Lagergren's pseudo first-order model	q_e (mg/g)	0.7797	0.5848	2.9029	0.9259
	k_1 (min^{-1})	0.0105	0.0108	0.0297	0.0219
	R^2	0.9374	0.9338	0.9671	0.9972
Pseudo second-order model	q_e (mg/g)	3.8655	4.1305	4.11	4.25
	k_2 (g/mg min)	0.0394	0.0557	0.020	0.048
	R^2	0.9998	0.9999	0.9993	1.000

experimental and theoretical values of q_e using the pseudo second-order kinetic model. Moreover, the R^2 values in all cases studied were nearly unity and even unity for AWSCC, which was indicative that the kinetics data fitted exceedingly well the pseudo second-order model for all adsorbents investigated. The pseudo second-order model can be considered as the rate-limiting (or determining) step and probably a chemical adsorption (chemisorption) involving valance forces through ion exchange between each metal ion and the active binding sites existed in WSC, AWSC, WSCC and AWSCC. The pseudo-second order kinetic model was also reported to fit well the kinetic data of the adsorption of Zn^{2+} ions onto pomelo peel (Saikaew et al., 2009), adsorption of Cu^{2+} ions onto Tectona grandis leaves (Kumar et al., 2006), adsorption of Pb^{2+} ions onto pumpkin seed shell activated carbon (Okoye et al., 2010), adsorption of Ni^{2+} ions onto potato peel (Prasad and Abdullah, 2009), and adsorption of Cr (VI) ions onto cooked tea dust (Dhanakumar et al., 2007).

The kinetic data were further analysed using the Boyd kinetics in order to determine the actual rate-controlling step involved in the Zn^{2+} ions adsorption process on WSC, AWSC, WSCC and AWSCC owing to the two mass transfer of solute (both film and pore diffusion). The Boyd kinetics (Boyd et al., 1947) is given by:

$$F = 1 - \frac{6}{\pi^2}\exp(-Bt) \quad (29)$$

$$Bt = -In(1-F) - 0.4977 \quad (30)$$

Where, $F\left(=q_t/q_e\right)$ is the fraction of solute adsorbed at time, *t*. The value of *B* was computed according to Eq. (28) for each value of *F* for each of the adsorbents used in this study, and then plotted against time to construct the Boyd plots (Ho et al., 2002) for the system under investigation, as depicted in Figure 9. The linearity of these plots was used to distinguish between external transport (film diffusion) and intraparticle transport controlled rates of adsorption (Wang et al., 2006). A straight line passing through the origin is indicative of adsorption process governed by intraparticle diffusion; otherwise it is governed by film diffusion (Mohan and Singh, 2002). From Figure 9, the plots for the four adsorbents studied were neither linear nor passed through the origin, which indicates that in all the adsorbents studied, film diffusion is the rate-determining adsorption process for Zn (II) ions on WSC, AWSC, WSCC and AWSCC as adsorbents. This is in conformity with the earlier result presented in Table 8 that a poor fit of the kinetic data was obtained for the IPD kinetic model.

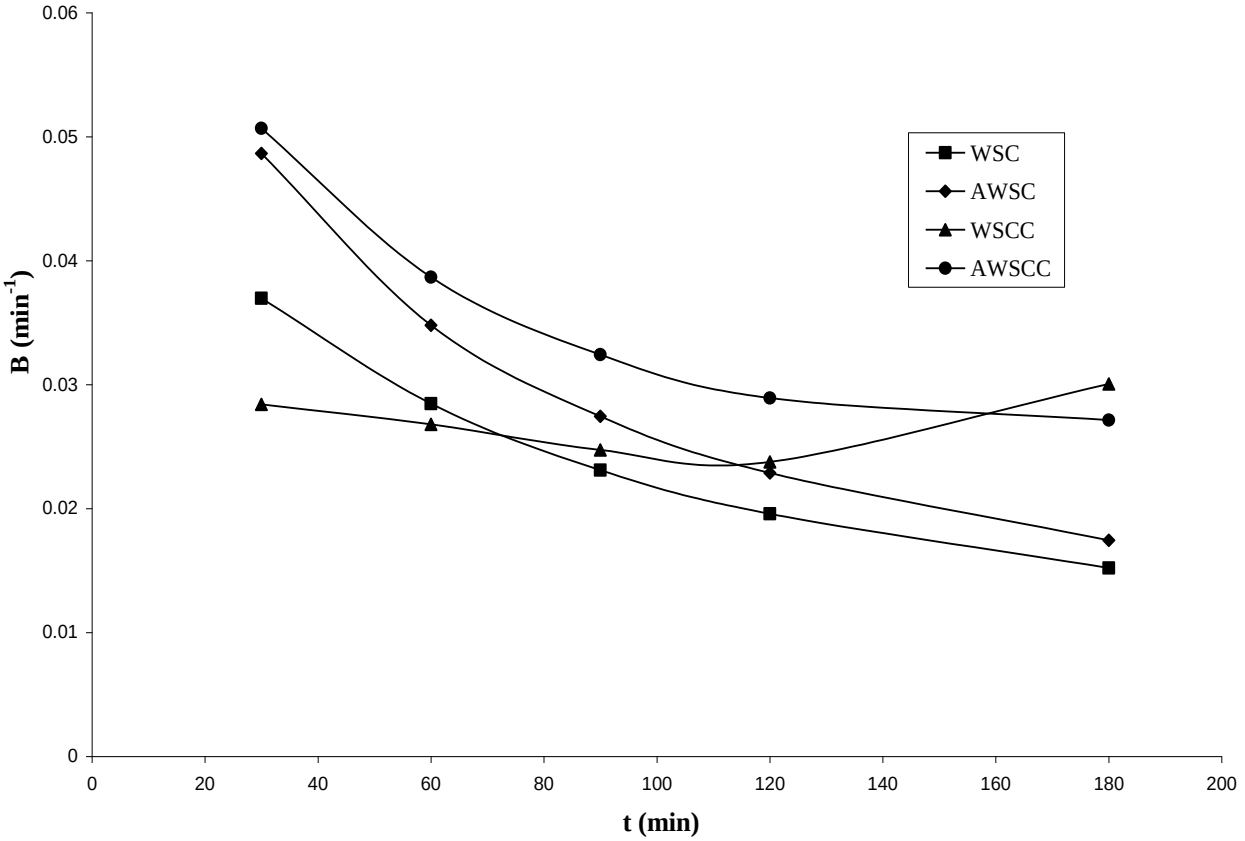

Figure 9. Boyd plots of the kinetic data for Zn (II) ions adsorption on WSC, AWSC, WSCC and AWSCC as adsorbents.

Thermodynamic studies of Zn (II) ions adsorption

Before investigating the thermodynamics of Zn (II) ions adsorption on the derived composite biosorbents from walnut shell, the effect of temperature on the % removal of Zn (II) ions from synthetic wastewater using WSC, AWSC, WSCC and AWSCC as adsorbents was studied. This is an important process for removal of heavy metals from industrial wastewater as effluents are produced at varying temperatures in industrial practice. Table 9 shows the effect of temperature on the % removal of Zn (II) ions, where the % removal of Zn (II) ions and equilibrium biosorption capacity decreased with increasing temperature. Hence, Zn (II) ions adsorption was exothermic in nature.

It was found that low temperature favours the removal of Zn (II) ions from wastewater for all the prepared biosorbents, with maximum % removal being 83.81, 78.81, 64.60 and 59.34 for WSC, AWSC, WSCC and AWSCC respectively at 303 K for pH=5, 1 g of adsorbent dosage, Zn (II) ions initial concentration of 100 mg/L, contact time of 2 h, agitation speed of 150 rpm and particle size of 60 BSS. The equilibrium adsorption capacity decreased at temperature below 303 K, which suggested the exothermic adsorption nature of Zn (II) ions onto the prepared composite biosorbents (Aksu and Tezer, 2005). Theoretically, % removal of Zn (II) ion on the prepared biosorbents decreases with increasing temperature owing to adsorption of already adsorbed ions (Zubair et al., 2008). The low % removal at higher temperatures may be due to the destruction of active binding sites (Witek-Krowiak, 2011).

Having established the temperature dependence of the Zn (II) ions removal, thermodynamics studies were carried out to comprehend wholly the nature of the adsorption process by computing changes in enthalpy, ΔH, entropy, ΔS and Gibbs free energy, ΔG. This is with a view of confirming the exothermicity of the Zn (II) ions adsorption on the prepared composite biosorbents, non-spontaneity and feasibility of the adsorption process under investigation. The thermodynamic equilibrium constant, K_c, was determined using the relation:

$$q_e = K_c c_e \quad (31)$$

and the change in Gibb's free energy was thus calculated by using:

Table 9. Effect of temperature on % removal of Zn (II) ions and equilibrium biosorption capacity.

T(K)	WSC		AWSC		WSCC		AWSCC	
	θ	q_e (mg/g)	θ	q_e (mg/g)	θ	q_e (mg/g)	θ	q_e (mg/g)
303	59.34	5.9340	64.60	6.4600	78.81	7.8810	83.81	8.3810
308	55.03	5.5000	59.96	6.0000	77.00	7.7000	82.00	8.2000
313	50.10	5.0000	57.02	5.7000	75.04	7.5000	80.00	8.0000
323	43.98	4.4000	52.00	5.2000	69.97	7.0000	76.00	7.6000
333	40.01	4.0000	45.98	4.6000	65.02	6.5000	71.00	7.1000

Table 10. Values of thermodynamic parameters for Zn (II) ions adsorption on prepared composite biosorbents.

T/K	WSC	AWSC	WSCC	AWSCC
	ΔG (kJ/mol)			
303	4.8482	4.2853	2.4916	1.6587
308	5.3824	4.8580	2.8021	2.0133
313	5.9920	5.2585	3.1331	2.3844
323	6.8310	5.9685	3.9081	3.0880
333	7.4974	6.8188	4.6610	3.8959
ΔH (kJ/mol)	-21.9539	-20.4117	-19.6535	-20.8050
ΔS (kJ/(mol K))	-0.0888	-0.0818	-0.0730	-0.0741

$$\Delta G = -RT\,In\,K_c \quad (32)$$

However, $\Delta G = \Delta H - T\Delta S = -RT\,In\,K_c$

so $$In\,K_c = \frac{\Delta S}{R} - \frac{\Delta H}{RT} \quad (33)$$

Setting $Y = In\,K_c$, $X_1 = T^{-1}$, $a_0 = \Delta S/R$, and $a_1 = -\Delta H/R$, equation (33) becomes:

$$Y = a_o + a_1 X_1 \quad (34)$$

The regression coefficients, a_0 and a_1 were determined using linear regression analysis for each of the prepared composite biosorbents, and the results obtained are as follows:

For WSC, $In\,K_c = 2640.6T^{-1} - 10.682$, $R^2 = 0.9792$

For AWSC, $In\,K_c = 2455.1T^{-1} - 9.8392$ $R^2 = 0.9913$

For WSCC, $In\,K_c = 2363.9T^{-1} - 8.7745$, $R^2 = 0.9979$

For AWSCC, $In\,K_c = 2502.4T^{-1} - 8.9116$, $R^2 = 0.9990$

Thus, values of ΔH and ΔS were computed for the Zn (II) ions adsorption on WSC, AWSC, WSCC and AWSCC as adsorbents, and the results presented in Table 10.

The ΔG values were positive at all temperatures investigated, which was an indication of the non-spontaneity of the adsorption of Zn (II) ions on WSC, AWSC, WSCC and AWSCC. Hence, the Zn (II) ions adsorption process was endogonic. The negative values of ΔH for all the prepared composite biosorbents was a confirmation of the exothermicity of the Zn (II) ions adsorption process. The negative values of ΔS for WSC, AWSC, WSCC and AWSCC used for Zn (II) ions adsorption suggested that randomness at the solid/solution interface decreased as a result of Zn (II) ions adsorption onto these adsorbents. However, ΔS^0 values for all the prepared adsorbents were nearly zero, implying equilibrium conditions were established during the adsorption experiment, and the limiting value of zero being reached only by a reversible process.

Conclusion

Composite biosorbents were derived from walnut and snail shells for the adsorption of Zn (II) ions from the synthetic industrial wastewater. Chemical activation using phosphoric acid improved the specific surface area of

walnut shell carbon (WSC) while impregnation of WSC and acid-treated walnut shell carbon (AWSC) on the chitosan derived from snail shell enhances further the specific surface areas of WSC and AWSC. The removal efficiencies of Zn (II) ions using the prepared adsorbents were effective in the acidic range. The composite adsorbent of AWSCC exhibited the most effective removal efficiency of Zn (II) ions from aqueous solution. The Langmuir adsorption isotherm fitted excellently the adsorption data of Zn (II) ions on WSC, AWSC, WSCC and AWSCC owing to the highest R^2 value obtained. Moreover, in all the adsorbents (WSC, AWSC, WSCC and AWSCC) used in this study, film-diffusion was the rate-limiting adsorption process for Zn (II) ions and the kinetic data were excellently correlated with the pseudo second-order kinetic model. The uses of walnut and snail shells from renewable resources to produce activated carbon and composite adsorbents potentially provide a less costly and tremendously efficient adsorbent. The thermodynamic studies revealed that Zn (II) ions adsorption on WSC, AWSC, WSCC and AWSCC was non-spontaneous, endogonic, exothermic and favourable at low temperature of 30^{o}C.

Notation

A_T, Temkin isotherm equilibrium binding constant, L/g; b_T, Temkin isotherm constant; c_e, metal ion concentration at equilibrium, mg/L; c_0, initial metal ion concentration, mg/L; c_t, metal ion concentration at time *t*, mg/L; ***C*,** intercept on q_t axis for IPD model, mg/g; k_{IPD}, intraparticle diffusion rate constant, mg/g min^{½}; k_1, Lagergren's pseudo first-order rate constant, min^{-1}; k_2, pseudo second-order rate constant, g/mg min; k_F, fractional power kinetic model constant, mg/g; K_F, Freundlich isotherm parameter, (mg/g).(mg/L)^{n}; K_L, Langmuir isotherm parameter, L/mg; m, mass of adsorbent, g; *n,* heterogeneity factor; ***N,*** exponent of fractional power kinetic model; q_e, amount of heavy metals adsorbed at equilibrium, mg/g; $q_{\max}$, maximum monolayer coverage capacities, mg/g; q_t, amount of heavy metals adsorbed at time *t*, mg/g; ***R,*** universal gas constant, J/mol K; R^2, coefficient of correlation; ***t,*** adsorption time, min; *T,* adsorption temperature, K; V, volume of aqueous solution in contact with the adsorbent, α, rate of adsorption at zero coverage, mg/g min; β, extent of surface coverage, g/mg; ρ_b, bulk density of adsorbent, g/mL; Φ_1, Temkin constant related to the heat of sorption, J/mol; ω, agitation speed, rpm.

CONFLICT OF INTERESTS

The authors have not declared any conflict of interests.

REFERENCES

Adesola B, Ogundipe K, Sangosanya KT, Akintola BD, Oluwa A, Hassan E (2016). Comparative study on the biosorption of Pb(II), Cd(II) and Zn(II) using Lemon grass (Cymbopogon citratus): kinetics, isotherms and thermodynamics. Chemical International 2:89-102.

Ahlam MF, Nida MS, Amma HA, Akl MA (2012). Biosorption studies of Cr (VI) ions from electroplating wastewater by walnut shell powder. American Journal of Environmental Engineering 2(6):188-195.

Ahmeda M, Marshall WE, Rao RM (1997). Potential of agricultural by product based activated carbon for use in raw sugar decolourisation. Journal of the Science of Food and Agriculture 75:117-124.

Akram M, Bhatti HN, Iqbal M, Noreen S, Sadaf S. (2017).Biocomposite efficiency for Cr(VI) adsorption: Kinetic, equilibrium and thermodynamics studies. Journal of Environmental Chemical Engineering 5:400-411.

Aksu Z, Tezer S (2005). Biosorption of reactive dyes on the green alga *Chlorella vulgaris*, Process Biochemistry 40:1347-1361.

Alzaydian AS (2009). Adsorption of methylene blue from aqueous solution onto a low-cost natural Jordanian Tripoli. American Journal of Applied Sciences 6 (6):1047-1058.

Amadi S, Ukpaka C. (2015). Role of molecular diffusion in the recovery of water flood residual oil. Chemical International 2:103-114.

American Society for Testing and Materials (ASTM) (2006). Standard test method for determination of iodine number for activated carbon. ASTM Philadelphia P A. 4607-94.

Amuda OS, Ibrahim AO (2006). Industrial wastewater treatment for chemical oxygen demand (COD) using natural material as adsorbent. African Journal of. Biotechnology 5(16):1483-1487.

Amuda OS, Giwa AA, Bello IA (2007). Removal of heavy metal from industrial wastewater using modified activated coconut shell carbon. Biochemical Engineering Journal 36(2):174-181.

Aremu DA, Olawuyi JF, Meshitsuka S, Sridhar MK, Oluwande PA (2002). Heavy metal analysis of ground water from Warri, Nigeria. International Journal of Environmental Health Research 12:261-272.

Argun ME, Dursun S (2006). Removal of heavy metal ions using chemically modified adsorbents. Journal of International Environmental Application and Science 1:27-38.

Babarinde A, Ogundipe K, Sangosanya KT, Akintola BD, Elizabeth Hassan AO (2016). Comparative study on the biosorption of Pb(II), Cd(II) and Zn(II) using Lemon grass (Cymbopogon citratus): kinetics, isotherms and thermodynamics. Chemical International 2:89-102.

Babarinde A, Onyiaocha GO (2016). Equilibrium sorption of divalent metal ions onto groundnut (Arachis hypogaea) shell: kinetics, isotherm and thermodynamics. Chemical International 2:37-46.

Babel S, Kurniawan TA (2004). Cr (VI) removal from synthetic wastewater using coconut shell charcoal and commercial activated carbon modified with oxidizing agent and/or chitosan. Chemosphere 54(7):951-967.

Baes GB, Mesmer RE (1976). Hydrolysis of Cations, John Wiley and Sons, New York.

Bamgbose JT, Adewuyi S, Bamgbose O, Adetoye AA (2010). Adsorption kinetics of cadmium and lead by chitosan. African Journal of Biotechnology 9(17):2560-2565.

Bhattacharyya KG, Sharma A (2004). Adsorption of Pb (II) from aqueous solution by Azadirachta indica (Neem) leaf powder. Journal of Hazardous Materials 113(1-3):97-109.

Bhattacharyya KG, Sharma J, Sharma A (2009). Azadirachta Indica leaf powder as a biosorbent for Ni (II) in aqueous medium. Journal of Hazardous Materials 165(1-3):271-278.

Boyd GE, Adamson AW, Myers LS (1947). The exchange adsorption of ions from aqueous solutions by organic zeolites 2. Journal of the American Chemical Society 69:2836-2847.

Cai J, Yang J, Du Y, Fan L, Qiu Y, Li J, Kennedy JF (2006). Enzymatic preparation of chitosan from the waste Aspergillus Níger mycelium of citric acid production plant. Carbohydrate Polymers 64:151-157.
Chen H, Zhao J, Dai G, Wu J, Yan H (2010). Adsorption characteristics of Pb (II) from aqueous solution onto a natural biosorbent fallen Cinnamomoum Camphora leaves. Desalination 262(1-3):174-182.
Cheremisnoff P, Ellerbusch F (1978). Carbon Adsorption Handbook. Ann Anbor Science Handbook Publishing Inc. 72:689-706.
Coughlin RW, Deshaies MR, Davis EM (1990). Preparation of chitosan for heavy metal removal, Environmental Progress 9:35-42.
Dash SN (2010). Preparation of carbonaceous heavy metal adsorbent from Shorea robusta leaf litter using phosphoric acid Impregnation. International Journal of Environmental Science 1(3):296-313.
Daud WMAW, Ali WSW (2004). Comparison on pore development of activated carbon produced from palm shell and coconut shell. Bioresource Technology 93:63-73.
Deans JR, Dixon BG (1992). Uptake of Pb^{2+} and Cu^{2+} by Novel Bioplolymers. Water Research. 26:469-479
Dhanakumar S, Solaraj G, Mohanraj R, Pattabhi S (2007). Removal of Cr (VI) from aqueous solution by adsorption using cooked tea dust. Indian Journal of Science and Technology 1:1-9.
Dilyana Z, Stoyanka S (2010). Isolation and characterization of chitin from marine sources in black sea. Annual Assen Zlatarov University, Burgas, Bulgaria 39(1):37-41.
Ding P, Huang K, Li G, Liu Y, Zeng W (2006). Kinetics of adsorption of Zn (II) ion on chitosan derivatives. International Journal of Biological Macromolecules 39:222-227.
Domszy JG, Roberts GAF (1985). Evaluation of infrared spectroscopic techniques for analysing chitosan. Macromolecular Chemistry and Physics186:1671-1682.
Erdem E, Karapinar N, Donat R (2004). The removal of heavy metal cations by natural zeolites. Journal of Colloid and Interface Science. 261:309-319.
Faria PCC, Orfao JJM, Pereira MFR (2004). Adsorption of anionic and cationic dyes on activated carbons with different surface chemistries. Water Research 38(6):2043-2052.
Firas HK, Aurelia CN (2015). Removal of copper ions from industrial wastewater using walnut shells as a natural adsorbent material. U.P.B. Scientific Bulletin 77(3):142-150.
Foo KY, Hameed BH (2010). Insights into the modelling of adsorption isotherm systems, Review. Chemical Engineering Journal 156:2-10.
Gergova K, Petrov N, Eser S (1994). Adsorption properties and microstructure of activated carbons produced from agricultural by-products by steam pyrolysis. Carbon 32:693-702.
Ghasemi M, Ghoreyshi AA, Younesi H, Khoshhal S (2015). Synthesis of a high characteristics activated carbon from walnut shell for the removal of Cr (VI) and Fe (II) from aqueous solution: Single and binary solutes adsorption. Iranian Journal of Engineering 12(4):28-43.
González JF, Román S, González-Garcia CM, Nabais JMV, Ortiz AL (2009). Porosity development in activated carbons prepared from walnut shells by carbon dioxide or steam activation. Industrial & Engineering Chemistry Research 48(16):7474-7481.
Guibal E, Saucedo I, Jansson-Charrier M, Delanghe B, Le Cloirec P (1994). Uranium and vanadium sorption by chitosan and derivatives. Water Science and Technology 30:183-192.
Hawari A, Rawajfih Z, Nsour N (2009). Equilibrium and thermodynamic analysis of zinc ions adsorption by olive oil mill solid residues. Journal of Hazardous Materials168:1284-1289.
Hiral A, Odani H, Nakajima A (1991). Determination of degree of deacetylation of chitosan by 1H NMR spectroscopy, Polymer Bulletin 26:87-93.
Ho YS, Mckay G (2000). The kinetics of sorption of divalent metal ions onto sphagnum moss peat. Water Research 34(3):735-742.
Ho YS, Porter JF, Mckay G (2002). Equilibrium isotherm studies for the biosorption of divalent metal ions onto peat, copper, nickel and lead Single Component Systems. Water, Air, and Soil Pollution 141:1-12.
Idowu EA (2015). Adsorption of selected heavy metals on activated carbon prepared from plantain (*Musa paradisiaca*.) peel. M.Sc. Thesis, Department of Chemistry, Ahmadu Bello University, Zaria, Nigeria.
Iqbal M (2016). Vicia faba bioassay for environmental toxicity monitoring: a review. Chemosphere 144:785-802.
Iqbal M, Bhatti IA (2015). Gamma radiation/H_2O_2 treatment of a nonylphenol ethoxylates: degradation, cytotoxicity, and mutagenicity evaluation. Journal of Hazardous Materials 299:351-360.
Iqbal M, Iqbal N, Bhatti IA, Ahmad N, Zahid M (2016). Response surface methodology application in optimization of cadmium adsorption by shoe waste: a good option of waste mitigation by waste. Ecological Engineering 88:265-275.
Iqbal M, Khera RA (2015). Adsorption of copper and lead in single and binary metal system onto Fumaria indica biomass. Chemistry International 1:157b-163b.
Iqbal M, Nisar J (2015). Cytotoxicity and mutagenicity evaluation of gamma radiation and hydrogen peroxide treated textile effluents using bioassays. Journal of Environmental Chemical Engineering 3:1912-1917
Iqbal M, Nisar J, Adil M, Abbas M, Riaz M, Tahir MA, Younus M, Shahid M (2017). Mutagenicity and cytotoxicity evaluation of photo-catalytically treated petroleum refinery wastewater using an array of bioassays. Chemosphere 168:590-598.
Isa MT, Ameh AO, Tijjani. M, Adama KK (2012). Extraction and characterization of chitin and chitosan from Nigerian shrimps. International Journal of Biological and Chemical Sciences 6(1):453-466.
Jamal MA, Muneer M, Iqbal M (2015). Photo-degradation of monoazo dye blue 13 using advanced oxidation process. Chemistry International 1:12-16.
Jang M, Kong B, Jeong Y, Hyung Lee C, Nah J (2004). Physicochemical characterization of α-chitin, β-chitin, and γ-chitin separated from natural resources. Journal of Polymer Science Part A: Polym. Chem. 42:3423-3432.
Jeyakumar RP, Chandrasekaran V (2014). Adsorption of lead (II) ions by activated carbons prepared from marine green algae: Equilibrium and kinetics studies. International Journal of Industrial Chemistry 5:10.
Kafia M, Surchi S (2011). Agricultural wastes as low cost adsorbents for Pb removal: Kinetics, equilibrium and thermodynamics. International Journal of Chemistry 3:103-111.
Karthikeyan R, Vijayalakshmi S, Balasubramanian T (2004). Seasonal distribution of heavy metals in the sediments from Uppanar Estuary (East coast of India). Journal of Aquatic Biology 19:119-122.
Kausar, A, Bhatti HN, Iqbal M, Ashraf A. (2017). Batch versus column modes for the adsorption of radioactive metal onto rice husk waste: conditions optimization through response surface methodology. Water Science and Technology 76(5):1035-1043.
Khan A, Muthukrishnan M, Guha B (2009). Sorption and transport modelling of hexavalent chromium on soil media, Journal of Hazardous Materials 174:444-453.
Kumar YP, King P, Prasad VSRK (2006). Equilibrium and kinetic studies for the biosorption system of copper (II) ion from aqueous solution using Tectona grandis leaves powder. Journal of Hazardous Materials 137:1211-1217.
Lin TF, Wu JK (2001). Adsorption of arsenite and arsenate within activated alumina grains: Equilibrium and kinetics. Water Research 35(8):2049-2057.
Lodi A, Solisio C, Converti A, Borghi M (1998). Cadmium, zinc, copper, silver and chromium (III) removal from wastewaters by Sphaerotilus Natans. Bioprocess Engineering 19:197-203.
Logan JA, Rosemarie Y (2002). An assessment of biofuel use and burning of agricultural waste in the developing world. Global biogeochemical cycles 1:108-119.
Mahboobeh M, Ameneh K, Elham H (2012). Role of modified activated carbon by H_3PO_4 or K_2CO_3 from natural adsorbent for removal of Pb (II) from aqueous solutions. Carbon Letters 13(2):115-120.
Martino AD, Sittinger M, Risbud MV (2005). Chitosan: A versatile biopolymer for orthopaedic tissue engineering, Biomaterials 5983-6002.
Mohan M, Pittman CU (2007). Arsenic removal from water/wastewater using adsorbents – A critical review. Journal of Hazardous Materials 142:1-53.
Mohan D, Singh KP (2002). Single- and Multi-component Adsorption of cadmium and zinc using activated carbon derived from bagasse – An Agricultural Waste. Water Research 36:2304-2315.

Mohanasrinivasan V, Mishra M, Paliwal JS, Singh S, Selvarajan E, Suganthi V, Subathra Devi C (2014). Studies on heavy metal removal efficiency and antibacterial activity of chitosan prepared from shrimp shell waste. Biotechnology 4:167-176

Mushtaq M, Bhatti HN, Iqbal M, Noreen S (2016). Eriobotrya japonica seed biocomposite efficiency for copper adsorption: isotherms, kinetics, thermodynamic and desorption studies. Journal of Environmental Management 176:21-33.

Muzzarelli RAA (1977). Chitin. Pergamon Press: Oxford.

Naeem H, Bhattia HN, Sadaf S, Iqbal M. (2017). Uranium remediation using modified *Vigna radiata* waste biomass. Appl. Radiation & Isotopes 123:94-101.

Nomanbhay SM, Palanisamy K (2005). Removal of heavy metal from industrial wastewater using chitosan coated oil palm shell charcoal. Electronic Journal of Biotechnology 8(1):43-53.

Nouren S, Bhatti HN, Iqbal M, Bibi I, Kamal S, Sadaf S, Sultan M, Kausar A, Safa Y (2017). By-product identification and phytotoxicity of biodegraded Direct Yellow 4 dye. Chemosphere 169:474-484.

Oboh I, Aluyor E, Audu.T (2009). Biosorption of heavy metal ions from aqueous solutions using a biomaterial. Leonardo Journal of Sciences 14:58-65.

Okoye AI, Ejikeme PM, Onukwuli OD (2010). Lead removal from wastewater using fluted pumpkin seed shell activated carbon: Adsorption modelling and kinetics. International Journal of Environmental Science and Technology 7(4):793-800.

Patel R, Kumar S, Verma A, Srivastava S (2017). Kinetic and thermodynamic properties of pharmaceutical drug (Gabapentin) by potassium bromate ($KBrO_3$) in presence of microamount of Ir (III) chloride as catalyst in acidic medium. Chemistry International 3:158-164.

Paul HC, Logde PT (2007). Polymer Chemistry, 2nd ed. Boca Raton: CRC pp. 336-339.

Prasad AGD, Abdullah MA (2009). Biosorption potential of potato peel waste for the removal of nickel from aqueous solutions: Equilibrium and kinetic studies. International Journal of Chemical Engineering Research 1(2):77-87.

Qureshi K, Ahmad M, Bhatti I, Iqbal M, Khan A (2015). Cytotoxicity reduction of wastewater treated by advanced oxidation process. Chemical International 1:53-59.

Rashid A, Bhatti HN, Iqbal M, Noreen S (2016). Fungal biomass composite with bentonite efficiency for nickel and zinc adsorption: a mechanistic study. Ecological Engineering 91:459-471.

Rinaudo M (2006). Chitin and chitosan: Properties and applications, Prog. Polymer Science 3:603-632.

Robertson JB, Van Soest PJ (1981). The Analysis of Dietary Fibre in Food, Marcel Dekker, New York.

Rumengan IFM, Suryanto E, Modaso R, Wullur S, Tallei TE, Limbong D (2014). Structural characteristics of chitin and chitosan isolated from the biomass of cultivated rotifer, *Brachionus rotundiformis*. International Journal of Fisheries and Aquatic Sciences 3(1):12-18.

Saikaew W, Kaewsarn P, Saikaew W (2009). Pomelo peel: agriculture waste for biosorption of cadmium ions from aqueous solution. World Academy of Science, Engineering and Technology 3:393-401.

Sayed M (2015). Efficient removal of phenol from aqueous solution by the pulsed high voltage discharge process in the presence of H_2O_2. Chemical International 1:81-86.

Schmuhl R, Krieg HM, Keizer K (2001). Adsorption of Cu (II) and Cr (VI) ions by chitosan: kinetics and equilibrium studies. Water South Africa 27(1):1-8.

Sneha P, Aiswarya J, Changam SS, Sanjay MC (2014). Extraction and purification of chitosan from chitin isolated from sea prawn. Asian Journal of Pharmaceutical and Clinical Research 7:201-204.

Tsezos M, Bell JP (1989). Comparison of the biosorption and desorption of hazardous organic pollutants by live and dead biomass. Water Research 23:561-568.

Ukpaka CP, Igwe FU (2017). Modeling of the velocity profile of a bioreactor: the concept of biochemical process. Chemical International 3:258-267

Ukpaka CP, Izonowei T (2017). Model prediction on the reliability of fixed bed reactor for ammonia production. Chemical International 3:46-57.

Vold IMN, Vårum KM, Guibal E, Smidsød O (2003). Binding of ions to chitosan - selectivity studies. Carbohydrate Polymer 54:471-477.

Volesky B (1990). Biosorption of heavy metals. In: bioadsorbents and biosorption of heavy metals. B. Volesky (ed.). CRC Press: Boca Raton, FL, pp. 221-238.

Wana MW, Kan C, Buenda D, Rogel B, Lourdesp M (2010). Adsorption of copper (II) and lead (II) ions from aqueous solutions on chitosan coated sand. Carbohydrate Polymer 80:891-899.

Wang XS, Qin Y, Li ZF (2006). Biosorption of zinc from aqueous solutions by rice bran: kinetics and equilibrium studies. Separation Science and Technology 41:747-758.

Witek-Krowiak A, Szafran RG, Modelski S (2011). Biosorption of heavy metals from aqueous solutions onto peanut shell as a low-cost biosorbent, Desalination 265:126-134.

Wu FC, Tseng RL, Juang RS (2002). Adsorption of dyes and humic acid from water using chitosan encapsulated activated carbon. Journal of Chemical Technology and Biotechnology 77:1260-1269.

Zarur JN, Tovar CT, Ortíz AV, Acevedo D, Tovar RT (2018). Thermodynamics, kinetics and equilibrium adsorption of Cr (VI) and Hg (II) in aqueous solution on corn husk (Zea Mays). International Journal of ChemTech Research 11(5):265-280.

Zhai Y, Wei X, Zeng O, Zhang D, Chu K (2004). Study of adsorbent derived from sewage sludge for the removal of Cd^{2+}, Ni^{2+} in aqueous solutions. Separation and Purification Technology 38:191-200.

Zubair A, Bhatti HN, Hanif MA, Shafqat F (2008). Kinetic and equilibrium modeling for Cr(III) and Cr(VI) removal from aqueous solutions by *Citrus reticulata* waste biomass. Water, Air, & Soil Pollution 191:305-318.